



Cite this: *Dalton Trans.*, 2021, **50**, 4859

Synthesis and characterization of new Pd(II) and Pt(II) complexes with 3-substituted 1-(2-pyridyl)imidazo[1,5-*a*]pyridine ligands†

Sara Pischedda,^{a,b} Sergio Stoccoro,^{a,b} Antonio Zucca,^{a,b} Giuseppe Sciortino,^c Fabrizio Ortu^{d,e} and Guy J. Clarkson^f

Several palladium(II) and platinum(II) complexes (**1–20**) of general formula $[M(L^n)(X)(Y)]$ [$M = Pd, X = Y = Cl$ (**1–Cl–4–Cl**), $X = Y = OAc$ (**1–OAc–4–OAc**); $M = Pt: X = Y = Cl$ (**5–8**); $M = Pd, X = Cl, Y = CH_3$ (**9–12**); $M = Pt, X = Cl, Y = CH_3$ (**13–16**) or $X = Y = CH_3$ (**17–20**); $n = 1–4$] have been synthesized by reaction of different Pd(II) and Pt(II) derivatives with various 3-substituted 1-(2-pyridyl)imidazo[1,5-*a*]pyridines; *i.e.* $L^n = 1-(2-pyridyl)-3-aryl$ imidazo[1,5-*a*]pyridine (aryl = Phenyl, L^1 ; 2-*o*-Tolyl, L^2 ; Mesityl, L^3) and 1-(2-pyridyl)-3-benzylimidazo[1,5-*a*]pyridine (L^4). Detailed spectroscopic investigation (including IR, mono- and bi-dimensional 1H NMR) and elemental analysis has been performed for all these species, allowing their complete characterization. L^n act as *N,N*-bidentate ligands and coordinate the metal centers in a chelate fashion through the pyridyl (N_{py}) and the pyridine-like nitrogen atom of the imidazo[1,5-*a*]pyridine group (N_{im}). The X-ray structural analysis performed on two of Pd(II) and three Pt(II) complexes, namely $[Pd(L^2)(CH_3)Cl]$ (**10**), $[Pd(L^3)(CH_3)Cl]$ (**11**) and $[Pt(L^1)Cl_2]$ (**5**), $[Pt(L^4)Cl_2]$ (**8**), $[Pt(L^2)(CH_3)Cl]$ (**14**) confirmed the spectroscopic and analytical data. Finally DFT studies unveiled the structural reasons behind the inertia of the synthesised compounds toward metalation, identified as the higher angle steric strain in comparison with the analogous bipyridine complexes.

Received 17th February 2021.
Accepted 16th March 2021

DOI: 10.1039/d1dt00546d

rsc.li/dalton

Introduction

The coordination chemistry of heavy d^8 transition metals (*e.g.* Ir(I), Pd(II), Pt(II), Au(III)) is dominated by the use of bidentate nitrogen donors as supporting ligands, wherein 2,2'-bipyridines and 1,10-phenanthrolines are the most important examples.¹ In particular, the extraordinary coordination properties of 2,2'-bipyridines in metal-catalyzed reactions² have led to a myriad of applications in a variety of fields, including macromolecular chemistry,³ supramolecular chemistry,⁴ materials chemistry,⁵ photochemistry⁶ and electrochemistry.⁷

Following our continuous interest in the study of the reactivity of bidentate nitrogen ligands,⁸ we decided to investigate the coordinating behaviour of a series of aromatic *N*-heterocyclic ligands containing the imidazo[1,5-*a*]pyridine skeleton (Fig. 1)⁹ *i.e.* 1-(2-pyridyl)-3-arylimidazo[1,5-*a*]pyridines and 1-(2-pyridyl)-3-benzylimidazo[1,5-*a*]pyridine.

The wealth of nitrogen heterocycles offer many intriguing possibilities for the development of bidentate nitrogen donors for the synergic tuning of structural and physicochemical properties of resulting complexes. In particular, 1-(2-pyridyl)imidazo[1,5-*a*]pyridines have emerged as an attractive new class of ligands, owing to their ability to act as bidentate donors by employing their pyridyl unit in conjunction with a

^aDipartimento di Chimica e Farmacia, Università degli Studi di Sassari, via Vienna 2, 07100 Sassari, Italy. E-mail: stoccoro@uniss.it

^bConsorzio Interuniversitario Reattività Chimica e Catalisi (CIRCC), Bari, Italy

^cInstitute of Chemical Research of Catalonia (ICIQ), Av. Països Catalans 16, 43007 Tarragona, Spain

^dSchool of Chemistry, University of Leicester, University Road, Leicester, LE1 7RH, UK

^eDepartment of Chemistry, University of Manchester, Oxford Road, Manchester, M13 9PL, UK

^fDepartment of Chemistry, University of Warwick, Gibbet Hill Road, Coventry CV4 7AL, UK

† Electronic supplementary information (ESI) available. CCDC 2061441–2061445. For ESI and crystallographic data in CIF or other electronic format see DOI: 10.1039/d1dt00546d

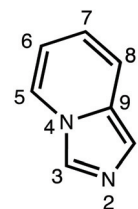


Fig. 1 Imidazo[1,5-*a*]pyridine skeleton: the atom numbering adopted throughout the text.

fused imidazole.¹⁰ Heterocycles containing the imidazo[1,5-*a*]pyridine skeleton possess unique photophysical properties¹¹ and have potential applications in the field of OLEDs¹² and organic thin-layer field-effect transistors (FETs).¹³ Different 1-(2-pyridyl)imidazo[1,5-*a*]pyridines have been coordinated to transition metals to produce highly luminescent complexes containing Re(III),¹⁴ Zn(II),^{13,15} Ag(I),¹⁶ Cd(II),¹⁷ Ru(II) and Os(II)¹⁸ metal centers. Furthermore, the coordination of these complexes with small organic molecules often produces a significant effect on their biological activities.¹⁹ The coordinating behaviour of these ligands with d⁸ ions of transition metals, like Pd(II) and Pt(II), is to our knowledge unexplored.

These ligands resemble 6-substituted 2,2'-bipyridines and we intended to verify the possibility that in addition to the typical N–N chelating behaviour (Fig. 2a), cyclometallated complexes could also be obtained by activation of a C–H bond of the aryl substituent in the 3-position (Fig. 2b), or *via* rollover cyclometallation resulting from the activation of a C–H bond of the pyridyl substituent (Fig. 2c).²⁰

With this idea in mind, we synthesized a series of ligands containing the heterocyclic imidazo[1,5-*a*]pyridine core, owing also to its huge biological and medicinal applications

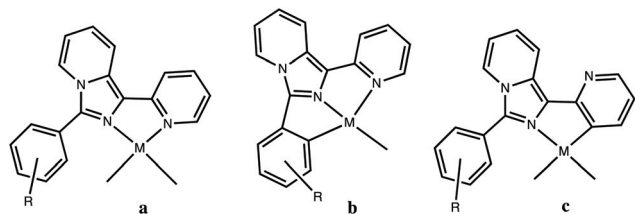


Fig. 2 Sketch of possible targets.

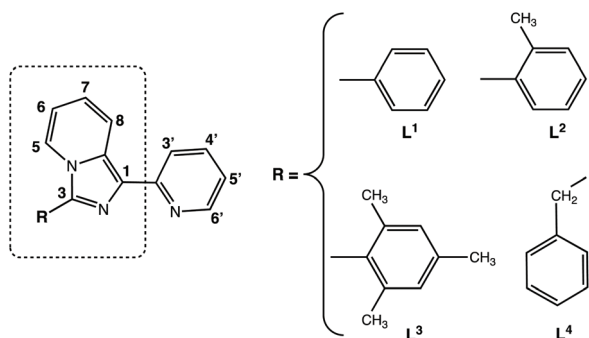


Fig. 3 Ligands synthesized and used in this work.

(Fig. 3).^{19–21} We also selected several substituents to tune the steric protection around the metal center and allow for different C–H activation possibilities involving either C(sp²)–H or C(sp³)–H bonds, thus leading to the potential formation of 5- and 6-membered metallacycles. Therefore, we selected aryls [phenyl (Ph, L¹), *o*-tolyl (*o*-Tol, L²), mesityl (Mes, L³)], together with a benzylic group (CH₂Ph, L⁴) as substituents.

Results and discussion

Synthesis and characterization of the ligands

The ligands 1-(2-pyridyl)-3-arylimidazo[1,5-*a*]pyridine L^{*n*} (*n* = 1–3) (Fig. 3) were readily synthesized, in good yields, by reacting suitable aromatic aldehydes with 2,2'-dipyridylketone and ammonium acetate in hot acetic acid, using minor modifications to the published procedures.²² On the other hand, the ligand 1-(2-pyridyl)-3-benzylimidazo[1,5-*a*]pyridine, L⁴, was synthesized following a different procedure due to the instability of the corresponding aliphatic imine which is formed during the synthesis.²³

The structure of the ligands was assessed by ¹H NMR spectroscopy: multi-dimensional NMR experiments were employed to assign all the proton signals (see Table 1).

For example, the interpretation of ¹H NMR spectra of L^{*n*} in CDCl₃ is far from trivial; the existence of three different spin systems involving two sets of protons and a variable number of protons depending on the 3-substituent was clearly identified by 2D NMR techniques (COSY, and NOE, see the ESI†).²⁴ For L¹ these spin systems include 4 (●), 4 (○), and 5 (◆) protons respectively (Fig. 4). This information however was not sufficient to unequivocally assign all signals in relation to the proposed molecular structure.

In the ¹H NMR spectrum of L¹ the signal resonating at lower fields has been attributed to the proton H8; this is an anomalous chemical shift, especially compared to the signal of the proton H5 and considering also the proximity to the nitrogen atom in 4-position of the imidazo[1,5-*a*]pyridine skeleton. We believe this unusual shift is due to the interaction of the proton H8 with the nitrogen atom of the pyridyl substituent in 1-position (Fig. 5).

To confirm this observation we synthesized the isomer of L¹ (1-phenyl-3-(2-pyridyl)-imidazo[1,5-*a*]pyridine), L¹ⁱ, in which the positions of the 2-pyridyl and the phenyl substituents have been exchanged (Fig. 5).²⁵ Gratifyingly, in the ¹H NMR spectrum of L¹ⁱ the most deshielded proton is proton H5, which is in agreement with the presence of a long-range N⋯H inter-

Table 1 ¹H NMR selected data of L^{*n*} in CDCl₃

L ^{<i>n</i>}	H ⁸	H ^{6'}	H ⁵	H ^{3'}	H ^{4'}	H ^{5'}	H ⁶	H ⁷	Others
L ¹	8.70; d	8.64; d	8.26; d	8.24; d	7.72; td	7.10; dd	6.92; dd	6.65; td	
L ²	8.71; d	8.64; d	7.64; d	8.23; d	7.70; t	7.09; dd	6.60; t	6.93; t	2.26; s, CH ₃
L ³	8.94; d	8.89; d	7.61; d	8.48; d	7.95; td	7.33; dd	6.82; dd	7.17; t	2.62; s, [3H] CH ₃ <i>para</i> . 2.27; s, [6H] CH ₃ <i>ortho</i>
L ⁴	8.62; d	8.60; d	7.59; d	8.17; d	7.71; td	7.07; dd	6.52; dd	6.84; t	4.51; s, CH ₂

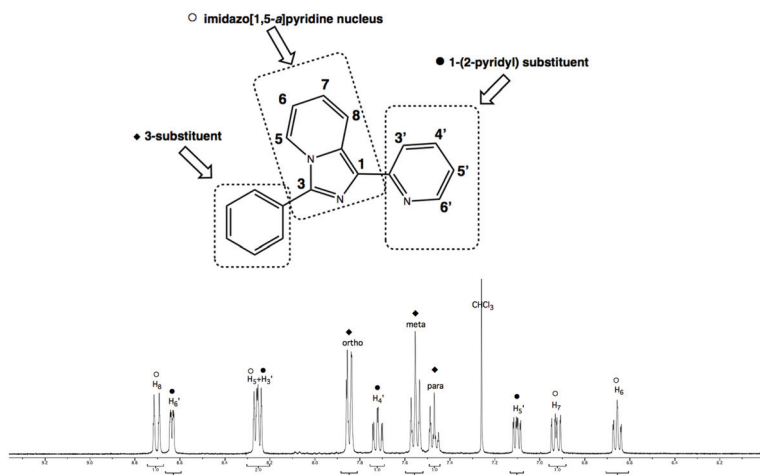


Fig. 4 Spin systems of ligand L^1 .

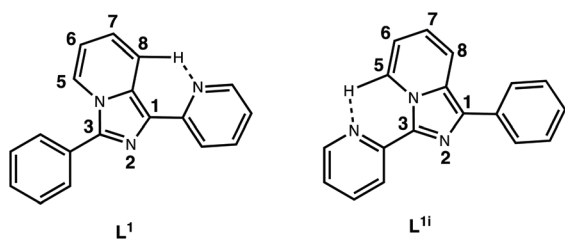


Fig. 5 Long-range $N\cdots H$ interaction in L^1 and L^{1i} .

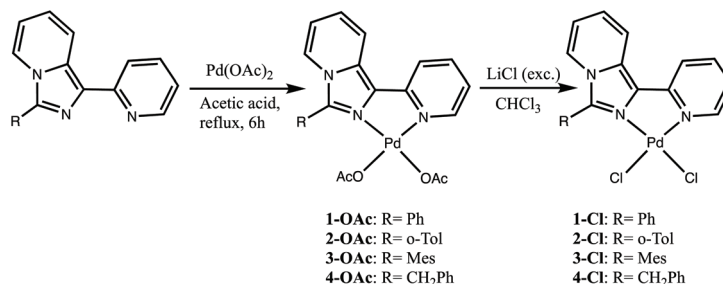
action (assignments based on COSY and NOESY spectra, Fig. S1†).

Synthesis and characterization of the complexes $[Pd(L^n)X_2]$ ($X = Cl, OAc$) and $[Pt(L^n)Cl_2]$

The reaction of L^{1-4} with $Pd(OAc)_2$ led to the formation of adducts $[Pd(L^n)(OAc)_2]$ (**1-OAc**: $n = 1$; **2-OAc**: $n = 2$; **3-OAc**: $n = 3$; **4-OAc**: $n = 4$), followed by anion exchange with $LiCl$ to yield the adducts $[Pd(L^n)Cl_2]$ (**1-Cl**: $n = 1$; **2-Cl**: $n = 2$; **3-Cl**: $n = 3$; **4-Cl**: $n = 4$). In all complexes the ligands act as classic chelating N^2N donors and spectroscopic investigation confirms the presence in solution of the $PdCl_2$ adducts, which was also further corroborated *via* elemental analysis (Scheme 1).

In the case of **1-Cl** the formation of a cyclometallated species can be ruled out by spectroscopic analysis, despite the employment of reaction conditions which normally afford activation of the $C(sp^2)-H$ bond in the *ortho* position of phenyl substituents.²⁶ In the 1H NMR spectrum of **1-Cl** the number of signals and their integral values are in perfect agreement with the proposed formulation. The most salient features are: (1) a significant upfield shift of the H8 signal upon complexation (δ 7.82 ppm *vs.* δ 8.70 ppm in the free ligand); (2) a downfield shift of the signal related to the proton H6' (δ 9.00 ppm *vs.* δ 8.61 ppm in the free ligand).

The alterations of the substituents in ligands L^2 , L^3 and L^4 offer different possibilities for the potential formation of cyclometalated species. With L^2 and L^3 ligands we wanted to exploit the possibility of the C–H activation in the methyl group in the *ortho* position, thereby leading to the formation of a 6-membered metallacycle featuring less ring strain with respect to analogous 5-membered cycles expected with L^1 . However, this would involve a less favourable activation of $C(sp^3)-H$ bonds compared to a $C(sp^2)-H$ activation predicted in the case of the phenyl substituent. On the other hand, the employment of ligand L^4 could lead to the formation of a 6-membered metallacycle by activating an aromatic $C(sp^2)-H$ bond. Nevertheless, in every case only the adducts $[Pd(L^n)Cl_2]$ were isolated and even trace amounts of the cyclometalated derivatives could not



Scheme 1 Synthesis of $PdCl_2$ adducts *via* metathesis of $Pd(OAc)_2$ adducts with $LiCl$.

Table 2 ^1H NMR data in CD_2Cl_2 of $[\text{Pd}(\text{L}^n)\text{Cl}_2]$ (**1-Cl–4-Cl**)

#	H ^{6'}	H ^{5'}	H ^{4'}	H ^{3'}	H ⁸	H ⁷	H ⁶	H ⁵	H ^{ar}	Other
1-Cl	9.10	7.22	7.85	7.98	7.91	7.33	6.89	7.97	7.65	
2-Cl	9.25	7.41	8.03	7.85	7.95	7.41	6.88	7.55	7.55–7.41	2.21 <i>ortho</i> CH ₃
3-Cl	9.26	7.33	8.01	7.43	7.93	7.33	6.87	7.84	7.08	2.41, <i>para</i> CH ₃ ; 2.03 <i>ortho</i> CH ₃ [6H]
4-Cl	9.27	7.27	7.97	7.89	7.89	7.27	6.88	7.77	7.34	4.44 CH ₂

Table 3 ^1H NMR data in CDCl_3 of $[\text{Pd}(\text{L}^n)(\text{OAc})_2]$ (**1-OAc–4-OAc**)

#	H ^{6'}	H ^{5'}	H ^{4'}	H ^{3'}	H ⁸	H ⁷	H ⁶	H ⁵	H ^{ar}	Other
1-OAc	8.12	7.24	7.98	7.80	7.91	7.29	6.86	7.85	7.67–7.60	1.99 CH ₃ (OAc); 1.13 CH ₃ (OAc)
2-OAc	8.14	7.25	7.98	7.51	7.89	7.31	6.86	7.79	7.50–7.40	2.18 <i>ortho</i> CH ₃ ; 1.98 CH ₃ (OAc); 1.11 CH ₃ (OAc)
3-OAc	8.14	7.30	7.98	7.40	7.89	7.24	6.85	7.77	7.04	2.35 <i>para</i> CH ₃ ; 2.09 <i>ortho</i> CH ₃ [6H]; 1.98 CH ₃ (OAc); 1.13 CH ₃ (OAc)
4-OAc	8.07	7.16	7.92	7.74	7.84	7.16	6.77	7.84	7.35–7.23	4.60 CH ₂ ; 2.14 CH ₃ (OAc); 1.89 CH ₃ (OAc)

be detected by ^1H NMR analysis. In the ^1H NMR spectra all signals have been assigned; noticeably, the proton H6' of the pyridyl ring is significantly deshielded, due to the presence of the chloride bound to the metal (Table 2).²⁷ The proposed structures were confirmed by CHN analyses.

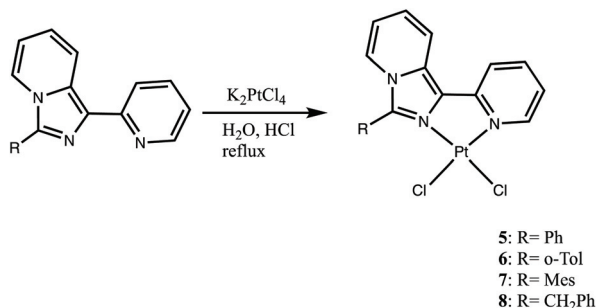
To confirm the lack of cyclometalated species, in the two steps process (see Scheme 1), the corresponding acetate derivatives **1-OAc**, **2-OAc**, **3-OAc** and **4-OAc** were also isolated and characterized. In the ^1H NMR spectra of these species (Table 3) different chemical shifts for methyl protons of the acetate are observed, likely due to the inequivalence of the two nitrogen donors. The methyl signal at higher fields can be confidently assigned as the acetate ligand in *trans* with respect to the pyridyl moiety (N_{py}): by arranging itself perpendicularly to the metal plane, the aromatic ring of the aryl group imparts a more effective shielding on the vicinal acetate group compared to the effect exerted on the other acetate ligand *trans* to the imidazolyl nitrogen (N_{im}). This effect is less pronounced in the case of **4-OAc** owing to the presence of the benzylic CH₂ spacer.

In order to further investigate the inertness towards metalation, we prepared the analogous Pt(II) from the reaction of ligands L^{1-4} with K_2PtCl_4 in a 1:1 ratio, in water and HCl under reflux (Scheme 2). These experimental conditions were chosen as they previously led to the formation of cyclometa-

lated species when 6-phenyl-2,2'-bipyridine was employed as a ligand.²⁸ However, also in this case only the corresponding Pt(II) adducts $[\text{Pt}(\text{L}^n)\text{Cl}_2]$ (**5**: $n = 1$; **6**: $n = 2$; **7**: $n = 3$; **8**: $n = 4$) could be isolated:

These were fully characterised with analytical and spectroscopic techniques; elemental analyses also support the formation of the adducts **5–8** and the absence of cyclometalated species. The ^1H NMR data is also in complete agreement with the proposed formulation. In particular, in all cases the H6 'proton signals are more deshielded than those of the corresponding palladium complexes most likely due to the greater electronegativity of platinum.²⁹ The coupling constant $^3J_{\text{Pt-H}}$ confirms the successful coordination of the pyridyl nitrogen to the platinum atom. In compound **7** the methyl groups in the *ortho* are isochronous, like in the case of the analogous Pd complex **3-Cl** (Table 4).

X-ray quality crystals of compounds **5** and **8** were obtained by slow diffusion of di-isopropyl ether into a dichloromethane solution at room temperature, which lead to the identification of the molecular structure of both species (Fig. 6). **5** and **8** crystallise in monoclinic $P2_1/n$ and $P2_1/c$ respectively, and both display square planar geometry around the Pt centre [**5**: $\Sigma_{\text{Z}} = 359.95(14)$; **8**: $\Sigma_{\text{Z}} = 360.0(2)^\circ$], featuring a pyridyl-imidazopyridine ligand which acts as a bidentate donor [**5**: Pt1–N1 = 2.020(2) Å, Pt1–N2 = 2.023(2) Å; **8**: Pt1–N1 2.029(2) Å, Pt1–N2 = 2.028(3) Å] and the metal centre perfectly placed on the mean plane calculated between the four donor atoms [Pt...mean l.s. plane: **5**: 0.0320(8) Å; **8**: 0.0109(11) Å]. Two chloride ions are bound to the metal centre in *cis* mutual position to complete the coordination sphere [**5**: Pt1–Cl1 = 2.2896(8) Å, Pt1–Cl2 = 2.2869(8) Å; **8**: Pt1–Cl1 = 2.2883(9) Å, Pt1–Cl2 = 2.2961(11) Å] (see Table S1†).

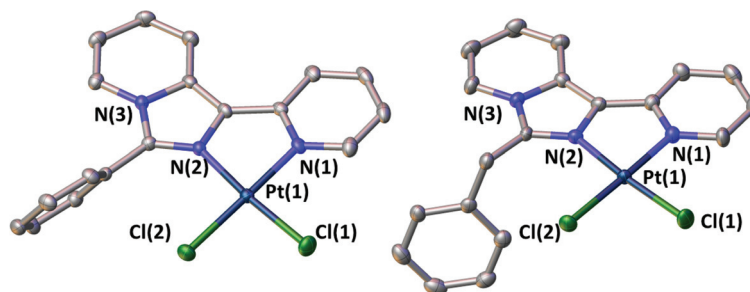
**Scheme 2** Synthesis of PtCl_2 adducts.

Synthesis of chloro(methyl) derivatives of Pd(II) and Pt(II), $[\text{M}(\text{L}^n)(\text{CH}_3)\text{Cl}]$

With the intent to further expand the coordination chemistry of these new ligands sets, we targeted the synthesis of heteroleptic adducts of Pd and Pt by employing the organometallic

Table 4 ^1H NMR data in CDCl_3 of $[\text{Pt}(\text{L}^n)\text{Cl}_2]$ (**5–8**)

#	$\text{H}^{6'}$	$\text{H}^{5'}$	$\text{H}^{4'}$	$\text{H}^{3'}$	H^8	H^7	H^6	H^5	H^{ar}	Other
5	9.51 (36 Hz) ^a	7.33	8.05	7.84	7.95	7.33	6.92	7.84	7.66	
6	9.63 (34 Hz)	7.62	8.07	7.86	7.96	7.62	6.91	7.62	7.62–7.28	2.22 <i>ortho</i> CH_3
7	9.63 (37 Hz)	7.31	8.07	7.87	7.97	7.37	6.91	7.43	7.07	2.42, <i>para</i> CH_3 ; 2.03, <i>ortho</i> CH_3 [6H]
8	9.39 (38 Hz)	7.51	8.22	8.22	8.33	7.22	7.12	8.33	7.51–7.22	5.41 CH_2

^a In brackets $^3J_{\text{Pt-H}}$.**Fig. 6** Solid state structure of **5** (left) and **8** (right) with selective atom labelling and thermal ellipsoids set at 50% probability level. Hydrogen atoms have been omitted for clarity. Selected bond length and angles for **5**: Pt(1)–Cl(1) 2.2896(8) (Å); Pt(1)–Cl(2) 2.2869(8) (Å); Pt(1)–N(1) 2.8020(2) (Å); Pt(1)–N(2) 2.023(2) (Å); N(1)–Pt(1)–N(2) 80.60(9)°. Selected bond length and angles for **8**: Pt(1)–Cl(1) 2.2883(8) (Å); Pt(1)–Cl(2) 2.2961(10) (Å); Pt(1)–N(1) 2.028(3) (Å); Pt(1)–N(2) 2.029(3) (Å); N(1)–Pt(1)–N(2) 80.44(11)°.

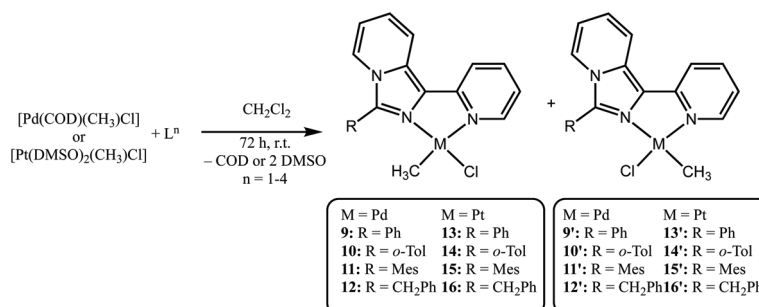
starting materials $[\text{Pd}(\text{COD})(\text{CH}_3)\text{Cl}]$ and $[\text{Pt}(\text{DMSO})_2(\text{CH}_3)\text{Cl}]$. These were reacted with the free ligands L^n (Scheme 3), affording the new heteroleptic organometallic derivatives $[\text{Pd}(\text{L}^n)(\text{CH}_3)\text{Cl}]$ (**9**: $n = 1$; **10**: $n = 2$; **11**: $n = 3$; **12**: $n = 4$) and $[\text{Pt}(\text{L}^n)(\text{CH}_3)\text{Cl}]$ (**13**: $n = 1$; **14**: $n = 2$; **15**: $n = 3$; **16**: $n = 4$).

All the resulting complexes are 1:1 adducts in which the nitrogen ligands act as a chelating donor. Due to the inequivalence of the two nitrogen donors and the planar square geometry typical of the Pd(II) and Pt(II) systems, two geometric isomers are expected: one with the methyl group in *trans* to pyridyl-N (N_{py}) the other with the methyl group in *trans* to imidazolyl-N (N_{im}) (Scheme 3). ^1H NMR studies (Table 5) reveal, in the case of most Pd complexes, there is a marked preference for the pyridyl donor (N_{py}) to bind *trans* to the methyl group (major isomers: **9–11**). The minor isomers, **9'–11'**, are also formed in smaller quantities, with the methyl groups positioned in *trans* with respect to the imidazolyl donor (N_{im}). In

Table 5 ^1H NMR selected data in CDCl_3 of $[\text{Pd}(\text{L}^n)(\text{CH}_3)\text{Cl}]$ (**9–12**) (**9'–12'**)

#	$\text{H}^{6'}$	CH_3 of the aryl substituent in 3 (L^2 , L^3) or CH_2 (L^4)	Pd- CH_3	%
9	9.11 d		0.35 s	85
9'	8.51 d		1.04 s	11
10	9.13 d	2.17 s [3H] <i>ortho</i>	0.39 s	95
10'	8.51 d	2.25 s	1.00 s	5
11	9.18 d	2.02 s [6H] <i>ortho</i> ; 2.41 s [3H] <i>para</i>	0.39 s	98
11'	8.55 d	2.03 s [6H] <i>ortho</i> ; 2.38 s [3H] <i>para</i>	1.01 s	2
12'	8.56 d	5.15 s [2H]	1.17 s	90
12	9.23 d	5.36 s [2H]	1.26 s	10

the ^1H NMR spectra of **9–11**, the signals related to the Pd- CH_3 and $\text{H}^{6'}$ pyridine protons are very diagnostic and indicate the formation of the proposed structures. In the major isomers $\delta(\text{Pd-Me})$ occurs in the range 1.05–0.35 ppm and the $\text{H}^{6'}$ are

**Scheme 3** Synthesis of heteroleptic organometallic Pd and Pt complexes **9–16** and isomers **9'–16'**.

markedly downfield shifted due to the proximity of the coordinated halide. In contrast, in the case of complex $[\text{Pd}(\text{L}^4)(\text{CH}_3)\text{Cl}]$ the major isomer in solution is that with the methyl group in *trans* to N_{im} (**12'**), most likely because of steric effects (*vide infra*).

The assignment of the two isomers' signals can be inferred from: (1) the chemical shift of the $\text{H}_{6'}$ proton, which is very deshielded compared to the free ligand, due to the presence of chloride bound to the metal center; (2) the chemical shift of the methyl ligand bound to the Pd centre, which is shielded by the proximity of the phenyl substituent that is located almost perpendicularly to the metal plane, thus shielding the methyl protons. In the case of complex $[\text{Pd}(\text{L}^1)(\text{CH}_3)\text{Cl}]$ a third species is also present (*ca.* 4%), which we assigned as the dichloride analogue **1**, occurring from the reaction of **9** with the chlorinated solvent.³⁰ The same trend can be reported for the other complexes, **10** and **11** with an increase in the percentage of the isomer prevailing (methyl ligand *trans* to pyridyl ring) with the increase in the steric hindrance of the substituent (Table 5).

The ^1H NMR spectrum of complex with L^4 displays a behaviour in stark contrast with our previous observations. The main stereoisomer is the one with the methyl in *trans* to the imidazo nitrogen (N_{im}) (**12'**), as it can be easily deduced by the chemical shift of the $\text{H}_{6'}$ proton (see Table 6). Because of the benzylic CH_2 spacer, the shielding effect operated by the aromatic ring of the substituent on the $\text{Pd}-\text{CH}_3$ is not as effective as that observed in the cases seen above (δ 1.26 ppm *vs.* δ 1.17 ppm).

X-ray quality crystals of compounds **10** and **11** were obtained by slow diffusion of di-isopropyl ether into a dichloromethane solution at room temperature (Fig. 7). Compound **10** crystallises in the monoclinic $P2_1/c$, whilst **11** crystallises in the triclinic $P\bar{1}$. Both compounds displays square planar geometries around the Pd centre [**10**: $\Sigma_{\angle} = 360.0(4)^\circ$; **11**: $\Sigma_{\angle} = 359.9(3)^\circ$], with the pyridyl-imidazopyridine ligands acting as bidentate donors similarly to what observed previously for **5** and **8** [**10**: $\text{Pd1}-\text{N1} = 2.143(5) \text{ \AA}$; $\text{Pd1}-\text{N2} = 2.067(5) \text{ \AA}$; **11**: $\text{Pd(1)}-\text{N(1)} = 2.055(3) \text{ \AA}$; $\text{Pd(1)}-\text{N(3)} = 2.148(4) \text{ \AA}$] and the metal centre perfectly placed on the mean calculated between the four donor atoms [Pt1...mean l.s. plane: **10**: 0.039(2) \AA ; **11**: 0.049(2) \AA]. In **10**, the methyl carbon C(20) is in the *trans* position with respect to pyridyl nitrogen N(3) [$\text{Pt1}-\text{C20} = 2.114(5) \text{ \AA}$], whilst chloride ion Cl(1) is positioned in *trans* to the imidazolyl nitrogen N(1) [$\text{Pt1}-\text{Cl1} = 2.295(2) \text{ \AA}$]. The same

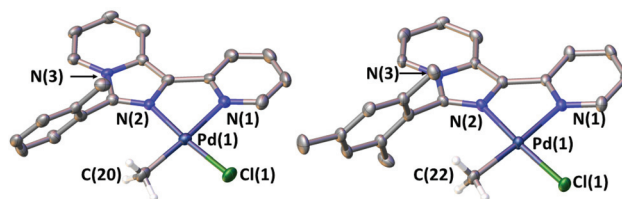


Fig. 7 Solid state structure of **10** (left) and **11** (right) with selective atom labelling and thermal ellipsoids set at 50% probability level. Hydrogen atoms have been omitted for clarity with the exception of those belonging to methyl groups C(20) and C(22). Selected bond length and angles for **10**: $\text{Pd(1)}-\text{Cl(1)} 2.300(2) \text{ \AA}$; $\text{Pd(1)}-\text{C(20)} 2.069(9) \text{ \AA}$; $\text{Pd(1)}-\text{N(1)} 2.147(4) \text{ \AA}$; $\text{Pd(1)}-\text{N(2)} 2.068(4) \text{ \AA}$; $\text{N(1)}-\text{Pd(1)}-\text{N(2)} 79.67(15)^\circ$. Selected bond length and angles for **11**: $\text{Pd(1)}-\text{Cl(1)} 2.3064(12) \text{ \AA}$; $\text{Pt(1)}-\text{C(22)} 2.049(5) \text{ \AA}$; $\text{Pd(1)}-\text{N(1)} 2.148(3) \text{ \AA}$; $\text{Pd(1)}-\text{N(2)} 2.055(3) \text{ \AA}$; $\text{N(1)}-\text{Pt(1)}-\text{N(2)} 78.94(12)^\circ$.

coordination motif is observed in **11** [$\text{Pd(1)}-\text{Cl(1)} = 2.3064(13) \text{ \AA}$; $\text{Pd(1)}-\text{C(22)} = 2.049(5) \text{ \AA}$; $\text{Cl(1)}-\text{Pd(1)}-\text{C(22A)} = 89.22(14)^\circ$] (see Table S2[†]). The isomers **10'** and **11'** were also detected as disordered components in the solid state analysis of **10** and **11**: **10'** has an occupancy of approximately 15%, whilst **11'** accounts for only 5% of the crystallographic model (see ESI[†]). These observations are in agreement with the spectroscopic data. Unfortunately, due to the low occupancy of the minor components (**10'** and **11'**), it is not possible to offer any detailed structural analysis.

In the case of Pt(*n*) analogue complexes $[\text{Pt}(\text{L}^n)(\text{CH}_3)\text{Cl}]$ (**13**: $n = 1$; **14**: $n = 2$; **15**: $n = 3$; **16**: $n = 4$) were obtained and characterised; the most significant data, obtained from the analysis of the ^1H NMR spectra, are reported in Table 6.

The Pt chloro(methyl)derivatives were obtained in good yield, with the exception of the complex obtained with L^4 (**16**). Also in this case all compounds were thoroughly characterized with analytical and spectroscopic methods. The interpretation of the ^1H NMR spectra of the platinum complexes (see Table 6) is simpler than palladium complexes due to the coupling of the protons with the NMR active ^{195}Pt nucleus. In this case, the Pt-H coupling allowed us to identify with certainty the prevailing geometric isomer in solution *i.e.* the one with N_{py} in *trans* to methyl group (**13**–**15**). Accordingly, the corresponding $^3J_{\text{Pt-H}}$ shown in Table 6 for the $\text{H}_{6'}$ signal of the pyridine ring should be very small, owing to the strong *trans*-influence the methyl ligand. In our case it was not possible to resolve these

Table 6 ^1H NMR selected data in CDCl_3 of $[\text{Pt}(\text{L}^n)(\text{CH}_3)\text{Cl}]$ (**13**, **14**, **15**; **13'**, **14'**, **16'**)

#	$\text{H}_{6'}$	CH_3 of the arylc substituent in 3 (L^2 , L^3) or CH_2 (L^4)	Pt- CH_3	%
13	9.49 d; (not resolved) ^a		0.51 s; $^2J_{\text{Pt-H}} = 78.1 \text{ Hz}$	80
13'	8.96 d; (<i>ca.</i> 60 Hz)		1.21 s; $^2J_{\text{Pt-H}} = 72.2 \text{ Hz}$	20
14	9.37d; (not resolved) ^a	2.04 s [3H] <i>ortho</i>	0.39 s; $^2J_{\text{Pt-H}} = 77.5 \text{ Hz}$	89
14'	8.84 d; (<i>ca.</i> 62 Hz)	2.12 s; [3H] <i>ortho</i>	1.09 s; $^2J_{\text{Pt-H}} = 71.7 \text{ Hz}$	11
15	9.44 d; (not resolved)	2.02 s [6H] <i>ortho</i> ; 2.19 s [3H] <i>para</i>	0.52 s; $^2J_{\text{Pt-H}} = 80.0 \text{ Hz}$	<i>ca.</i> 100
16'	9.04 d $^3J_{\text{Pt-H}} = 60.0 \text{ Hz}$	5.30 s [2H]	1.25 s; $^2J_{\text{Pt-H}} = 80.1 \text{ Hz}$	100

^a In brackets $^3J_{\text{Pt-H}}$.

signals due to the high intensity of the field to which the ^1H NMR spectra were registered (due to Chemical Shift Anisotropy, CSA). In the case of the minor isomer (*i.e.* with the methyl in *trans* to N_{im}) the value of $^3J_{\text{Pt-H}}$ for the same proton ($\text{H6}'$) was found to be approximately 60 Hz, which is in agreement with the presence in the *trans* position of a ligand with low *trans*-influence, such as a chloride. Also in this case, the chemical shift of the methyl ligand is considerably shielded by the ring current of the aryl substituent and resonates at $\delta = 1$ ppm, as already observed for the corresponding Pd complexes. When ligand L^4 was employed, complex $\mathbf{16}'$ was isolated in poor yield, featuring the methyl group in *trans* to N_{im} . In this case, the chemical shift of methyl is shifted to $\delta = 1.25$ ppm with a coupling constant of approximately 80 Hz. This observation highlights the effect of the benzylic CH_2 spacer in attenuating the shielding effect imparted by the aromatic ring of the substituent.

X-ray quality crystals of compound $\mathbf{14}$, were obtained by slow diffusion of di-isopropyl ether into a dichloromethane solution at room temperature (Fig. 8). Compound $\mathbf{14}$ crystallises in the monoclinic $P2_1/c$ and displays an analogous coordination motif to $\mathbf{10}$ and $\mathbf{11}$, with square planar geometry around the Pt centre [$\Sigma_{\text{Z}} = 360.0(6)^\circ$; Pt1–N1 = 2.110(4) Å; Pt1–N2 = 2.026(4) Å; Pt1...mean l.s. plane = 0.043(2) Å]; the Pt– $\text{N}_{\text{pyridyl}}$ distance is elongated with respect to dichloride analogues $\mathbf{5}$ and $\mathbf{8}$ [2.020(2) Å and 2.028(3) Å respectively] owing to the methyl carbon C(20) positioned in *trans* with respect to pyridyl nitrogen N(1) [Pt1–C20 = 2.068(11) Å], whilst the Pt–Cl

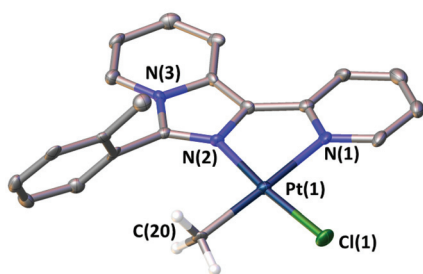


Fig. 8 Molecular structure of $\mathbf{14}$ with ellipsoids set at 50% probability level. Hydrogens have been omitted for clarity with the exception of those belonging to methyl group C(20).

bond is *trans* to the imidazo nitrogen N(2) is of similar magnitude to the other complexes described in this report [Pt1–Cl1 = 2.217(8) Å] (see Table S2†). Also in this case the isomer $\mathbf{14}'$ is present in the crystallographic model, with an occupancy of approximately 15% (see ESI†).

Synthesis of dimethyl derivatives of Pt(n), $[\text{Pt}(\text{L}^n)(\text{CH}_3)_2]$

Finally, we synthesised and fully characterised a series of dimethyl derivatives of formula $[\text{Pt}(\text{L}^n)(\text{CH}_3)_2]$ ($\mathbf{17}$: $n = 1$; $\mathbf{18}$: $n = 2$; $\mathbf{19}$: $n = 3$; $\mathbf{20}$: $n = 4$), by reacting the precursor $[\text{Pt}(\text{DMSO})_2(\text{CH}_3)_2]$ with free ligand L^n . Reactions were carried out initially in dichloromethane, but the solvent was changed to acetone in order to prevent activation of the chlorinated solvents as previously reported in the literature.³⁰ Indeed the ^1H NMR spectra recorded in CD_2Cl_2 showed evidence of a mixture of products consisting of the expected adduct, $[\text{Pt}(\text{L}^n)(\text{CH}_3)_2]$, together with a mixture of complexes obtained by oxidative addition of dichloromethane *i.e.* $[\text{Pt}(\text{L}^n)(\text{CH}_3)_2(\text{CH}_2\text{Cl})\text{Cl}]$.³⁰ So clean adducts were obtained by operating in acetone, and their formation was confirmed *via* ^1H NMR studies carried out in deuterated acetone (Table 7).

The elemental analyses and the spectroscopic characterization of these complexes are in agreement with the reported stoichiometry. The ligands act as a chelating bidentate with the two methyls in *trans* to the two different nitrogen atoms, N_{py} and N_{im} . The corresponding signals are easily distinguishable thanks to the chemical shift, being the one at higher fields the methyl in *trans* to the pyridine ring due to the screen operated by the substituent in 3-position of the imidazo-pyridine skeleton. This effect is less pronounced for the complex obtained with L^4 ($\mathbf{20}$). The $^3J_{\text{Pt-H}}$ of the protons belonging to the two methyl ligands coordinated to the Pt centre are not very different from each other, highlighting a very similar *trans*-influence of the two types of nitrogen donor groups. Surprisingly, the $^3J_{\text{Pt-H}}$ coupling constants of the $\text{H6}'$ protons can be accurately measured, unlike the platinum chloro (methyl) complexes seen previously (Table 7).

Theoretical analysis

As discussed above with this series of ligands, contrary to what was observed in our previous works,⁸ⁱ cyclometalation can't be realized. Taking advantage of the X-Ray structure of the $[\text{Pt}(\text{L}^n)\text{Cl}_2]$ series and to understand the nature of this phenomenon

Table 7 ^1H NMR in acetone- d_6 of $[\text{Pt}(\text{L}^n)(\text{CH}_3)_2]$ ($\mathbf{17}$ – $\mathbf{20}$)

#	$\text{H6}'$	CH_3 of the aryllic substituent in 3 (L^2 – L^3) or CH_2 (L^4)	Pt– CH_3
17	9.04 d; (<i>ca.</i> 24 Hz) ^a		0.76 s; $^3J_{\text{Pt-H}} = 90.0$ Hz 0.26 s; $^3J_{\text{Pt-H}} = 89.4$ Hz
18	9.03 d; (<i>ca.</i> 24 Hz)	2.21 s [3H] CH_3 <i>ortho</i>	0.75 s; $^3J_{\text{Pt-H}} = 88.5$ Hz 0.24 s; $^3J_{\text{Pt-H}} = 90.6$ Hz
19	9.04 d; (<i>ca.</i> 24 Hz)	2.38 s [3H] CH_3 <i>para</i> ; 2.01 s [6H] CH_3 <i>ortho</i>	0.77 s; $^3J_{\text{Pt-H}} = 88.1$ Hz 0.28 s; $^3J_{\text{Pt-H}} = 88.5$ Hz
20	9.04 d; (<i>ca.</i> 24 Hz)	4.90 s, [2H]	1.10 s; $^3J_{\text{Pt-H}} = 87.0$ Hz 0.91 s; $^3J_{\text{Pt-H}} = 87.9$ Hz

^a In brackets $^3J_{\text{Pt-H}}$.

Table 8 Theoretical relative ΔG_{aq} calculations for the cyclometallation reaction of the synthesized adducts: $[(\text{Pt}(\text{L}^n)\text{Cl}_2)_{\text{aq}}] \rightarrow [(\text{Pt}(\text{L}^n\text{-H})\text{Cl})_{\text{aq}}] + \text{HCl}_{\text{aq}}$

Complex	$\Delta\Delta G_{\text{gas}}^a$	$\Delta\Delta G_{\text{aq}}^{a,b}$
$[(\text{Pt}(\text{L}^1\text{-H})\text{Cl})]$	21.15	17.31
$[(\text{Pt}(\text{L}^2\text{-H})\text{Cl})]$	16.84	13.41
$[(\text{Pt}(\text{L}^3\text{-H})\text{Cl})]$	14.08	11.12
$[(\text{Pt}(\text{L}^4\text{-H})\text{Cl})]$	13.97	7.10

^a Values in kcal mol⁻¹ referred to the value obtained for the bipy complex taken as a zero, ref. 8i. ^b Gibbs free energy computed with the following formulae: $\Delta G_{\text{aq}} = \Delta G_{\text{gas}} + \Delta G_{\text{sol}}([(\text{Pt}(\text{L}^n\text{-H})\text{Cl})]) - \Delta G_{\text{sol}}([(\text{Pt}(\text{L}^n)\text{Cl}_2)]) + \Delta G_{\text{sol}}(\text{HCl}) + RT \ln V$.

we performed a theoretical prediction of the Gibbs energy associated with the metalation of the four Pt adducts $[(\text{Pt}(\text{L}^n)\text{Cl}_2)_{\text{aq}}] \rightarrow [(\text{Pt}(\text{L}^n\text{-H})\text{Cl})_{\text{aq}}] + \text{HCl}_{\text{aq}}$ comparing the values with the thermodynamics of the complex formed by the similar ligand 6-(1-phenylbenzyl)-2,2'-bipyridine (bipy). In Table S5† is summarized a comparison of X-Ray and DFT (M06/6-311g(d, p)/SDD+f[ECP]) selected parameters, the little deviations demonstrate that the selected DFT level of theory guarantees accurate performances in the structural prediction of this kind of complexes. Furthermore the method appear robust and was successfully applied in literature for high accuracy energy prediction of transition metal complexes.³¹

The results summarized in Table 8 clearly show that the hypothetical reaction is associated, for all the ligands, with ΔG_{aq} values considerably higher respect the homologous reaction of $[(\text{Pt}(\text{bipy})\text{Cl}_2)]$. Particularly $\Delta\Delta G_{\text{aq}}$ values ranging from 7.10 to 17.31 kcal mol⁻¹ highlight thermodynamics inertia of the metallation for the $[(\text{Pt}(\text{L}^n)\text{Cl}_2)]$ series.

An accurate structural analysis of the hypothetical cyclometallated complexes unveils the reasons behind the high $\Delta\Delta G_{\text{aq}}$ associated with the cyclometallation. The 5-member and 6-member rings formed by the ligands L^{1-4} presents a high angle steric strain in comparison with the characterized bipyridine complex. As it can be seen in Table 9, the mean of the deviation from the ideal angles ranges from 4.35° to 8.51° for the ligands synthesized in this work *versus* 2.94° computed for the stable complex $[\text{Pt}(\text{bipy}\text{-H})\text{Cl}]$. In addition, the distances Pt(II)-N play a critical role, in fact the cyclometallation forces these bonds to become smaller respect to the ideal values increasing the potential energy of the compounds.

Conclusions

In this work we wanted to test the behaviour of four ligands of the imidazo[1,5a]pyridine series with Pd(II) and Pt(II) in order to compare the results with those obtained with 2,2'-bipyridine ligands. Although this study with these metal ions is a novelty for these ligands, the result is that only neutral adducts have been obtained in which the ligand acts as an N,N chelator: in no case has activation of CH bonds been obtained as was obtained instead in the case of 2,2'-bipyridine ligands. The theoretical study performed on the Pt(II) series suggests that the high angle steric strain of the 5- and 6-membered rings formed by the ligands L^{1-4} as well as the deviation from ideal Pt(II)-N distances could be responsible of the thermodynamics inertia of these complexes toward cyclometallation.

Table 9 Selected bond lengths and bond angles on the formed ring in cyclometallation reaction. In parenthesis is reported the absolute deviation from the ideal value in angstrom and degrees respectively

	$[\text{Pt}(\text{L}^1\text{-H})\text{Cl}]^a$	$[\text{Pt}(\text{L}^2\text{-H})\text{Cl}]^a$	$[\text{Pt}(\text{L}^3\text{-H})\text{Cl}]^a$	$[\text{Pt}(\text{L}^4\text{-H})\text{Cl}]^a$	$[\text{Pt}(\text{bipy}\text{-H})\text{Cl}]^a$
Angles ^{b,c}					
1-2-3	5-member ring 112.05 (7.95)	6-member ring 116.88 (7.38)	6-member ring 116.44 (6.94)	6-member ring 123.61 (3.61)	6-member ring 120.27 (0.27)
2-3-4	114.18 (5.82)	125.44 (5.44)	124.73 (4.73)	127.76 (7.76)	122.70 (2.70)
3-4-5	113.93 (6.07)	120.29 (0.29)	118.29 (1.71)	118.64 (9.14)	115.51 (6.01)
4-5-1(6)	126.28 (6.28)	123.28 (3.28)	123.22 (3.22)	126.37 (6.37)	119.34 (0.66)
5-1(6)-2(1)	73.56 (16.44)	130.11 (10.11)	128.79 (8.79)	131.17 (11.17)	124.30 (4.30)
6-1-2	—	90.36 (0.36)	89.28 (0.72)	92.09 (2.09)	93.67 (3.67)
Mean dev.	8.51	4.48	4.35	6.69	2.94
Distances ^{b,c}					
Pt(II)-N(1)	1.933 (0.090)	1.978 (0.045)	1.980 (0.043)	1.982 (0.041)	2.041 (0.018)
Pt(II)-N(3)	2.313 (0.293)	2.198 (0.178)	2.211 (0.191)	2.196 (0.176)	2.154 (0.134)
Mean dev.	0.192	0.112	0.117	0.109	0.076

^a DFT computed structural data from this work. ^b Angles in degrees. ^c Distances in Å.

Experimental section

All the solvents were purified and dried according to standard procedures.³² The starting complexes $[\text{Pd}(\text{COD})(\text{CH}_3)\text{Cl}]$,³³ *trans*- $[\text{Pt}(\text{DMSO})_2(\text{CH}_3)\text{Cl}]$ ³⁴ and *cis*- $[\text{Pt}(\text{DMSO})_2(\text{CH}_3)_2]$ ^{26a,35} were synthesized according to literature. Elemental analyses were performed with a Perkin-Elmer elemental analyzer 240B at the Department of Chemistry and Pharmacy of the University of Sassari. FT-IR spectra were registered with a Jasco FT-IR-480 Plus spectrometer. ¹H spectra were recorded with a Bruker Avance III 400 spectrometer operating at 400.0 MHz. Chemical shifts are given in ppm relative to internal TMS for ¹H, J values are given in Hz. Two-dimensional ¹H COSY and NOESY spectra were performed by means of standard pulse sequences.

Synthesis of the ligands

L¹ (3-phenyl-1-(pyridin-2-yl)imidazo[1,5-a]pyridine). To a solution of bis(2-pyridyl)ketone (0.9209 g; 5.00 mmol) in acetic acid (30 ml) were added benzaldehyde (1.01 ml; 10 mmol) and ammonium acetate (1.9010 g; 25 mmol). The pale yellow solution was refluxed under inert atmosphere for 5 h. The solution was then put in a mixture of water/ice (250 ml), extracted with dichloromethane. Dried with Na₂SO₄, filtered and concentrated to small volume. The product was purified with a chromatographic column using a mixture of ethyl acetate and *n*-hexane (8 : 2). The solution was concentrated to a small volume and *n*-hexane was added to give a yellow precipitate (**L¹**). Yield: 0.6647 g (49%).

¹H NMR, δ_{H} [CDCl_3]: 8.70 (d, 1H, **H⁸**); 8.64 (d, 1H, **H⁶**); 8.26 (d, 1H, **H⁵**); 8.24 (d, 1H, **H³**); 7.85 (dd, 2H, **ortho H**); 7.72 (td, 1H, **H⁴**); 7.54 (td, 2H, **meta H**); 7.47 (tt, 1H, **para H**); 7.10 (dd, 1H, **H⁵**); 6.92 (dd, 1H, **H⁷**); 6.65 (td, 1H, **H⁶**).

¹H NMR, δ_{H} [CD_2Cl_2]: 8.71 (d, 1H, **H⁸**); 8.61 (d, 1H, **H⁶**); 8.30 (d, 1H, **H³**); 8.21 (d, 1H, **H⁵**); 7.85 (d, 2H, **ortho H**); 7.74 (t, 1H, **H⁴**); 7.58 (t, 2H, **meta H**); 7.49 (t, 1H, **para H**); 7.11 (dd, 1H, **H⁵**); 6.95 (td, 1H, **H⁷**); 6.61 (dd, 1H, **H⁶**).

¹H NMR, δ_{H} [$(\text{CD}_3)_2\text{CO}$]: 8.74 (d, 1H, **H⁸**); 8.62 (d, 1H, **H⁶**); 8.50 (d, 1H, **H⁵**); 8.26 (d, 1H, **H³**); 7.94 (d, 2H, **ortho H**); 7.80 (td, 1H, **H⁴**); 7.60 (t, 2H, **meta H**); 7.51 (t, 1H, **para H**); 7.16 (dd, 1H, **H⁵**); 7.04 (dd, 1H, **H⁷**); 6.84 (t, 1H, **H⁶**).

L² (3-(*o*-tolyl)-1-(pyridin-2-yl)imidazo[1,5-a]pyridine). To a solution of bis(2-pyridyl)ketone (0.9209 g; 5.00 mmol) in acetic acid (30 ml) were added *o*-tolylaldehyde (1.20 ml; 10 mmol) and ammonium acetate (1.9003 g; 25 mmol). The pale yellow solution was refluxed under inert atmosphere for 5 h. The solution was then put in a mixture of water/ice (250 ml), extracted with dichloromethane, dried with Na₂SO₄, filtered and concentrated to small volume. The product was purified with a chromatographic column using a mixture of ethyl acetate and *n*-hexane (8 : 2). The solution was concentrated to a small volume and *n*-hexane was added to give a yellow precipitate (**L²**). Yield: 0.8560 g (60%).

¹H NMR, δ_{H} [CDCl_3]: 8.71 (d, 1H, **H⁸**); 8.64 (d, 1H, **H⁶**); 8.23 (d, 1H, **H³**); 7.70 (t, 1H, **H⁴**); 7.64 (d, 1H, **H⁵**); 7.51 (d, 1H, **H⁶**);

7.40 (m, 3H, **H^{5'}** + **H^{4'}** + **H^{3'}**); 7.09 (t, 1H, **H⁵**); 6.93 (dd, 1H, **H⁷**); 6.60 (t, 1H, **H⁶**), 2.26 (s, 3H, **CH₃**).

¹H NMR, δ_{H} [CD_2Cl_2]: 8.71 (d, 1H, **H⁸**); 8.63 (d, 1H, **H⁶**); 8.20 (d, 1H, **H³**); 7.73 (t, 1H, **H⁴**); 7.69 (d, 1H, **H⁵**); 7.51 (d, 1H, **H⁶**); 7.42 (m, 3H, **H^{5'}** + **H^{4'}** + **H^{3'}**); 7.11 (t, 1H, **H⁵**); 6.96 (t, 1H, **H⁷**); 6.65 (t, 1H, **H⁶**), 2.27 (s, 3H, **CH₃**).

¹H NMR, δ_{H} [$(\text{CD}_3)_2\text{CO}$]: 8.72 (d, 1H, **H⁸**); 8.62 (d, 1H, **H⁶**); 8.21 (d, 1H, **H³**); 7.85 (d, 1H, **H⁵**); 7.78 (td, 1H, **H⁴**); 7.56 (d, 1H, **H⁶**); 7.44 (m, 3H, **H^{5'}** + **H^{4'}** + **H^{3'}**); 7.15 (dd, 1H, **H⁵**); 7.03 (dd, 1H, **H⁷**); 6.78 (t, 1H, **H⁶**), 2.27 (s, 3H, **CH₃**).

L³ (3-mesityl-1-(pyridin-2-yl)imidazo[1,5-a]pyridine). To a solution of bis(2-pyridyl)ketone (0.9207 g; 5.00 mmol) in acetic acid (30 ml) were added mesitylaldehyde (1.04 ml; 10 mmol) and ammonium acetate (1.9023 g; 25 mmol). The pale yellow solution was refluxed under inert atmosphere for 5 h. The solution was then put in a mixture of water/ice (250 ml), extracted with dichloromethane, dried with Na₂SO₄, filtered and concentrated to small volume. The product was purified with a chromatographic column using a mixture of ethyl acetate and *n*-hexane (8 : 2). The solution was concentrated to a small volume and *n*-hexane was added to give a yellow precipitate (**L³**). Yield: 0.9088 g (58%).

¹H NMR, δ_{H} [CDCl_3]: 8.94 (d, 1H, **H⁸**); 8.89 (d, 1H, **H⁶**); 8.48 (d, 1H, **H³**); 7.95 (td, 1H, **H⁴**); 7.61 (d, 1H, **H⁵**); 7.33 (dd, 1H, **H⁵**); 7.26 (s, 2H, **meta H**); 7.17 (dd, 1H, **H⁷**); 6.82 (td, 1H, **H⁶**); 2.62 (s, 3H, **para CH₃**); 2.27 (s, 6H, **ortho CH₃**).

¹H NMR, δ_{H} [CD_2Cl_2]: 8.68 (d, 1H, **H⁸**); 8.62 (d, 1H, **H⁶**); 8.20 (d, 1H, **H³**); 7.72 (t, 1H, **H⁴**); 7.36 (d, 1H, **H⁵**); 7.09 (t, 1H, **H⁵**); 7.05 (s, 2H, **meta H**); 6.93 (t, 1H, **H⁶**); 6.60 (t, 1H, **H⁷**); 2.38 (s, 3H, **para CH₃**); 1.99 (s, 3H, **ortho CH₃**).

¹H NMR, δ_{H} [$(\text{CD}_3)_2\text{CO}$]: 8.71 (d, 1H, **H⁸**); 8.62 (d, 1H, **H⁶**); 8.20 (d, 1H, **H³**); 7.77 (td, 1H, **H⁴**); 7.51 (d, 1H, **H⁵**); 7.14 (dd, 1H, **H⁵**); 7.08 (s, 2H, **meta H**); 7.02 (dd, 1H, **H⁷**); 6.75 (t, 1H, **H⁶**); 2.37 (s, 3H, **para CH₃**); 1.99 (s, 6H, **ortho CH₃**).

L⁴ (3-benzyl-1-(pyridin-2-yl)imidazo[1,5-a]pyridine). To a solution of bis(2-pyridyl)ketone (1.3998 g; 7.60 mmol) in methanol (30 ml) were added phenylalanine (1.2554 g; 7.6 mmol) and slowly a few drops of acetic acid. The pale yellow solution was refluxed in an inert atmosphere for 12 h. The resulting orange solution was concentrated to a small volume and diethyl ether added to give a product which was purified with a chromatographic column using a mixture of ethyl acetate and *n*-hexane (8 : 2). The solution was evaporated completely to give **L⁴** as a brown oil. Yield: 1.4963 g (69%).

¹H NMR, δ_{H} [CDCl_3]: 8.62 (d, 1H, **H⁶**); 8.60 (d, 1H, **H⁸**); 8.17 (d, 1H, **H³**); 7.71 (td, 1H, **H⁴**); 7.59 (d, 1H, **H⁵**); 7.24 (m, 5H, **H^{ar}**); 7.07 (dd, 1H, **H⁵**); 6.84 (dd, 1H, **H⁷**); 6.52 (t, 1H, **H⁶**); 4.51 (s, 2H, **CH₂**).

¹H NMR, δ_{H} [CD_2Cl_2]: 8.62 (d, 1H, **H⁸**); 8.60 (d, 1H, **H⁶**); 8.16 (d, 1H, **H³**); 7.73 (t, 1H, **H⁴**); 7.68 (d, 1H, **H⁵**); 7.27 (m, 5H, **H^{ar}**); 7.10 (t, 1H, **H⁵**); 6.88 (t, 1H, **H⁷**); 6.59 (t, 1H, **H⁶**); 4.49 (s, 2H, **CH₂**).

¹H NMR, δ_{H} [CD_3COCD_3]: 8.62 (d, 1H, **H⁸**); 8.58 (d, 1H, **H⁶**); 8.20 (d, 1H, **H³**); 8.03 (d, 1H, **H⁵**); 8.02 (t, 1H, **H⁴**); 7.25 (m, 5H, **H^{ar}**); 7.12 (dd, 1H, **H⁵**); 6.92 (dd, 1H, **H⁷**); 6.69 (t, 1H, **H⁶**); 4.52 (s, 2H, **CH₂**).

$^1\text{H NMR}$, δ_{H} [(CD₃)₂SO]: 8.56 (d, 1H, H⁶); 8.47 (d, 1H, H⁸); 8.16 (d, 1H, H⁵); 8.05 (d, 1H, H³); 7.78 (t, 1H, H⁴); 7.27 (s, br 5H, H^{ar}); 7.17 (dd, 1H, H⁵); 6.97 (t, 1H, H⁷); 6.75 (t, 1H, H⁶); 4.48 (s, 2H, CH₂).

L¹¹ (1-phenyl-3-(pyridin-2-yl)imidazo[1,5-a] pyridine). To a solution of 2-benzoylpyridine (0.9160 g; 5 mmol) in toluene (25 ml) were added benzyl ammine (950 μL ; 5.5 mmol), iodide (1.5302 g; 6 mmol) and sodium acetate (1.2302 g; 15 mmol). The dark solution was refluxed in an inert atmosphere for 6 h, until to disappear of the ketone. At the solution was added Na₂SO₃ (5%) and the mixture was extracted with dichloro methane and water. The organic fraction was anhydriified with Na₂SO₄ and filtered. The product was purified with a chromatographic column using a mixture of ethyl acetate and petroleum ether (1 : 3) and obtained as a yellow precipitate (**L¹¹**). Yield: 0.5964 g (44%).

$^1\text{H NMR}$, δ_{H} [CDCl₃]: 10.03 (d, 1H, H⁵); 8.65 (d, 1H, H⁶); 8.49 (d, 1H, H³); 7.97 (d, 2H, *ortho* H); 7.90 (d, 1H, H⁸); 7.79 (td, 1H, H⁴); 7.49 (t, 2H, *meta* H); 7.32 (t, 1H, *para* H); 7.21 (dd, 1H, H⁵); 6.94 (dd, 1H, H⁷); 6.77 (t, 1H, H⁶).

$^1\text{H NMR}$, δ_{H} [CD₃COCD₃]: 10.08 (d, 1H, H⁵); 8.695 (d, 1H, H⁶); 8.48 (d, 1H, H⁸); 8.04 (m, 3H, *ortho* H + H³); 7.93 (td, 1H, H⁴); 7.49 (t, 2H, *meta* H); 7.33 (t, 1H, *para* H + H⁵); 7.07 (t, 1H, H⁶); 6.91 (t, 1H, H⁷).

$^1\text{H NMR}$, δ_{H} [(CD₃)₂SO]: 9.97 (d, 1H, H⁵); 8.715 (d, 1H, H⁶); 8.10 (d, 1H, H⁸); 8.04 (m, 3H, *ortho* H + H³); 7.51 (t, 2H, H^{ar}); 7.39 (t, 1H, H⁴); 7.33 (t, 1H, H⁵); 7.11 (t, 1H, H⁶); 6.99 (t, 1H, H⁷).

Synthesis of the complexes

[Pd(L¹)Cl₂] (1-Cl). To a solution of L¹ (0.1193 g; 0.44 mmol) in acetic acid (25 ml) was added Pd(OAc)₂ (0.0988 g; 0.44 mmol). The orange solution was refluxed under an inert atmosphere for 6 h and evaporated to dryness. The crude obtained was solubilized with chloroform (25 ml), treated with LiCl in excess, stirred for 12 h at room temperature then filtered. The resulting solution was concentrated to a small volume and diethyl ether added to give a precipitate which was recrystallized from CH₂Cl₂/Et₂O to give the analytical sample as yellow solid (**1-Cl**). Yield: 0.0947 g (48%). M.p.: 276 °C.

Found: C 47.85; H 2.80; N 9.25%. Calc. for C₁₈H₁₃Cl₂N₃Pd: C, 48.19; H, 2.92; N, 9.37.

$^1\text{H NMR}$, δ_{H} [CD₂Cl₂]: 9.10 (d, 1H, H⁶); 7.98 (d, 1H, H³); 7.97 (t, 2H, H⁵); 7.91 (d, 1H, H⁸); 7.85 (t, 1H, H⁴); 7.65 (m, 5H, H^{ar}); 7.33 (d, 1H, H⁷); 7.22 (t, 1H, H⁵); 6.89 (t, 1H, H⁶).

[Pd(L²)Cl₂] (2-Cl). To a solution of L² (0.1259 g; 0.44 mmol) in acetic acid (25 ml) was added Pd(OAc)₂ (0.0987 g; 0.44 mmol). The orange solution was refluxed under an inert atmosphere for 6 h and evaporated to dryness. The crude obtained was solubilized with chloroform (25 ml), treated with LiCl in excess, stirred for 12 h at room temperature then filtered. The resulting solution was concentrated to a small volume and diethyl ether added to give a precipitate which was recrystallized from CH₂Cl₂/Et₂O to give the analytical sample as yellow solid (**2-Cl**). Yield: 0.0997 g (49%). M.p.: 215 °C.

Found: C 49.30; H 2.99; N 8.94%. Calc. for C₁₉H₁₅Cl₂N₃Pd: C, 49.32; H, 3.27; N, 9.08.

$^1\text{H NMR}$, δ_{H} [CD₂Cl₂]: 9.25 (d, 1H, H⁶); 8.03 (t, 1H, H⁴); 7.95 (d, 1H, H⁸); 7.85 (d, 1H, H³); 7.55 (m, 2H, H^{6'} + H⁵); 7.41 (m, 5H, H^{5''} + H^{4''} + H^{3''} + H^{5'} + H⁷); 6.88 (t, 1H, H⁶); 2.21 (s, 3H, CH₃).

[Pd(L³)Cl₂] (3-Cl). To a solution of L³ (0.1391 g; 0.44 mmol) in acetic acid (25 ml) was added Pd(OAc)₂ (0.0988 g; 0.44 mmol). The orange solution was refluxed under an inert atmosphere for 6 h and evaporated to dryness. The crude obtained was solubilized with chloroform (25 ml), treated with LiCl in excess, stirred for 12 h at room temperature then filtered. The resulting solution was concentrated to a small volume and diethyl ether added to give a precipitate which was recrystallized from CH₂Cl₂/Et₂O to give the analytical sample as yellow solid (**3-Cl**). Yield: 0.1900 g (88%). M.p.: >290 °C.

Found: C 51.04; H 3.50; N 8.46%. Calc. for C₂₁H₁₉Cl₂N₃Pd: C, 51.40; H, 3.90; N, 8.56.

$^1\text{H NMR}$, δ_{H} [CD₂Cl₂]: 9.26 (d, 1H, H⁶); 8.01 (t, 1H, H⁴); 7.93 (d, 1H, H⁸); 7.84 (d, 1H, H⁵); 7.43 (d, 1H, H³); 7.33 (m, 2H, H^{5'} + H⁷); 7.08 (s, 2H, *meta* H); 6.87 (t, 1H, H⁶); 2.41 (s, 3H, *para* CH₃); 2.03 (s, 6H, *ortho* CH₃).

[Pd(L⁴)Cl₂] (4-Cl). To a solution of L⁴ (0.1251 g; 0.44 mmol) in acetic acid (50 ml) was added Pd(OAc)₂ (0.0989 g; 0.44 mmol). The solution was refluxed under an inert atmosphere for 6 h and evaporated to dryness. The crude obtained was solubilized with chloroform (25 ml), treated with LiCl in excess, stirred for 12 h at room temperature then filtered. The resulting solution was concentrated to a small volume and diethyl ether added to give a precipitate which was recrystallized from CH₂Cl₂/Et₂O to give the analytical sample as yellow solid (**4-Cl**). Yield: 0.0631 g (31%). M.p.: 225 °C.

Found: C 49.30; H 2.99; N 8.90%. Calc. for C₁₉H₁₅Cl₂N₃Pd: C, 49.32; H, 3.27; N, 9.08.

$^1\text{H NMR}$, δ_{H} [CD₂Cl₂]: 9.27 (d, 1H, H⁶); 7.97 (t, 1H, H⁴); 7.89 (m, 2H, H⁸ + H³); 7.77 (d, 1H, H⁵); 7.34 (m, 5H, H^{ar}); 7.27 (m, 2H, H^{5'} + H⁷); 6.88 (t, 1H, H⁶); 4.44 (broad, 2H, CH₂).

[Pd(L¹)(OAc)₂] (1-OAc). To a solution of L¹ (0.1193 g; 0.44 mmol) in dichloromethane (25 ml) was added Pd(OAc)₂ (0.0988 g; 0.44 mmol). The orange solution was stirred for 12 h at room temperature, then evaporated to a small volume and diethyl ether added. The yellow precipitate formed was filtered off and recrystallized from CH₂Cl₂/Et₂O to give the analytical sample as a yellow solid (**1-OAc**). Yield: 0.2050 g (94%). M.p.: 176 °C.

Found: C 52.95; H 3.74; N 8.30%. Calc. for C₂₂H₁₉N₃O₄Pd: C, 53.29; H, 3.86; N, 8.47.

$^1\text{H NMR}$, δ_{H} [CD₂Cl₂]: 8.12 (d, 1H, H⁶); 7.98 (td, 1H, H⁴); 7.91 (d, 1H, H⁸); 7.85 (d, 1H, H⁵); 7.80 (d, 1H, H³); 7.67–7.60 (m, 5H, H^{ar}); 7.29 (dd, 1H, H⁷); 7.24 (t, 1H, H⁵); 6.86 (t, 1H, H⁶); 1.99 (s, 3H, C(O)CH₃); 1.13 (s, 3H, C(O)CH₃).

[Pd(L²)(OAc)₂] (2-OAc). To a solution of L² (0.1259 g; 0.44 mmol) in dichloromethane (25 ml) was added Pd(OAc)₂ (0.0987 g; 0.44 mmol). The orange solution was stirred for 12 h at room temperature, then evaporated to a small volume and diethyl ether added. The yellow-green precipitate was filtered

off and recrystallized from CH₂Cl₂/Et₂O to give the analytical sample as yellow solid (**2-OAc**). Yield: 0.0919 g (41%). M.p.: 250 °C.

Found: C 53.90; H 3.95; N 7.99%. Calc. for C₂₃H₂₁N₃O₄Pd: C, 54.18; H, 4.15; N, 8.24.

¹H NMR, δ_H [CD₂Cl₂]: 8.14 (d, 1H, H⁶); 7.98 (d, 1H, H⁴); 7.89 (d, 1H, H⁸); 7.79 (d, 1H, H⁵); 7.51 (d, 1H, H³); 7.50–7.40 (m, 4H, H^{ar}); 7.31 (t, 1H, H⁷); 7.25 (t, 1H, H⁵); 6.86 (t, 1H, H⁶); 2.26 (s, 3H, *ortho* CH₃); 1.98 (s, 3H, C(O)CH₃); 1.11 (s, 3H, C(O)CH₃).

[Pd(L³)(OAc)₂] (**3-OAc**). To a solution of L³ (0.1383 g; 0.44 mmol) in dichloromethane (25 ml) was added Pd(OAc)₂ (0.0985 g; 0.44 mmol). The orange solution was stirred for 12 h at room temperature, then evaporated to a small volume and diethyl ether added. The yellow precipitate formed was filtered off and recrystallized from CH₂Cl₂/Et₂O to give the analytical sample as a yellow solid (**3-OAc**). Yield: 0.2130 g (90%). M.p.: 268 °C.

Found: C 55.01; H 4.15; N 7.64%. Calc. for C₂₅H₂₅N₃O₄Pd: C, 55.82; H, 4.68; N, 7.81.

¹H NMR, δ_H [CD₂Cl₂]: 8.14 (d, 1H, H⁶); 7.98 (t, 1H, H⁴); 7.89 (d, 1H, H⁸); 7.77 (d, 1H, H⁵); 7.40 (d, 1H, H³); 7.30 (t, 1H, H⁵); 7.24 (t, 1H, H⁷); 7.04 (s, 2H, *meta* H); 6.85 (t, 1H, H⁶); 2.35 (s, 3H, *para* CH₃); 2.09 (s, 6H, *ortho* CH₃); 1.98 (s, 3H, C(O)CH₃); 1.13 (s, 3H, C(O)CH₃).

[Pd(L⁴)(OAc)₂] (**4-OAc**). To a solution of L⁴ (0.1259 g; 0.44 mmol) in dichloromethane (25 ml) was added Pd(OAc)₂ (0.0986 g; 0.44 mmol). The orange solution was stirred for 12 h at room temperature, then evaporated to a small volume and diethyl ether added. The yellow precipitate formed was filtered off and recrystallized from CH₂Cl₂/Et₂O to give the analytical sample as a yellow solid (**4-OAc**). Yield: 0.1435 g (64%). M.p.: 260 °C.

Found: C 53.90; H 3.94; N 8.02%. Calc. for C₂₃H₂₁N₃O₄Pd: C, 54.18; H, 4.15; N, 8.24.

¹H NMR, δ_H [CD₂Cl₂]: 8.07 (d, 1H, H⁶); 7.92 (t, 1H, H⁴); 7.84 (t, 2H, H⁵ + H⁸); 7.74 (d, 1H, H³); 7.35–7.23 (m, 5H, H^{ar}); 7.16 (m, 2H, H⁵ + H⁷); 6.77 (t, 1H, H⁶); 4.61 (s, 2H, CH₂); 2.10 (s, 3H, Pd-CH₃); 1.73 (s, 3H, Pd-CH₃).

[Pt(L¹)Cl₂] (**5**). To a solution of K₂PtCl₄ (0.1005 g; 0.24 mmol) in H₂O (25 ml) were added L¹ (0.0651 g; 0.24 mmol) and slowly few drops of HCl (2 M). The mixture was heated at reflux under an inert atmosphere for 72 h, until the solution was colourless, and then cooled. The yellow precipitate was filtered off, washed with water, ethanol and diethyl ether and finally recrystallised from dichloromethane and diethyl ether to give the analytical sample as a yellow solid (**5**). Yield: 0.1225 g (95%). M.p.: > 290 °C.

Found: C 39.97; H 2.10; N 7.63%. Calc. for C₁₈H₁₃Cl₂N₃Pt: C, 40.24; H, 2.44; N, 7.82.

¹H NMR, δ_H [CD₂Cl₂]: 9.51 (d, 1H, ³J_{Pt-H} = 36 Hz, H⁶); 8.05 (t, 1H, H⁴); 7.95 (d, 1H, H⁸); 7.84 (m, 2H, H³ + H⁵); 7.66 (m, 5H, H^{ar}); 7.33 (m, 2H, H⁵ + H⁷); 6.92 (t, 1H, H⁶).

[Pt(L²)Cl₂] (**6**). To a solution of K₂PtCl₄ (0.1001 g; 0.24 mmol) in H₂O (25 ml) were added L² (0.0687 g; 0.24 mmol) and slowly few drops of HCl (2 M). The mixture

was heated at reflux under an inert atmosphere for 72 h, until the solution was colourless, and then cooled. The yellow precipitate was filtered off, washed with water, ethanol and diethyl ether and finally recrystallised from dichloromethane and diethyl ether to give the analytical sample as a yellow solid (**6**). Yield: 0.0793 g (60%). M.p.: > 290 °C.

Found: C 41.01; H 2.53; N 7.44%. Calc. for C₁₉H₁₅Cl₂N₃Pt: C, 41.39; H, 2.74; N, 7.62.

¹H NMR, δ_H [CD₂Cl₂]: 9.63 (d, 1H, ³J_{Pt-H} = 34 Hz, H⁶); 8.07 (t, 1H, H⁴); 7.96 (d, 1H, H⁸); 7.86 (d, 1H, H³); 7.62–7.28 (m, 7H, H⁵ + H^{Ar} + H⁵ + H⁷); 6.91 (t, 1H, H⁶); 2.22 (s, 3H, CH₃).

[Pt(L³)Cl₂] (**7**). To a solution of K₂PtCl₄ (0.1002 g; 0.24 mmol) in H₂O (25 ml) were added L³ (0.0754 g; 0.24 mmol) and slowly few drops of HCl (2 M). The mixture was heated at reflux under an inert atmosphere for 72 h, until the solution was colourless, and then cooled. The yellow precipitate was filtered off, washed with water, ethanol and diethyl ether and finally recrystallised from dichloromethane and diethyl ether to give the analytical sample as a yellow solid (**7**). Yield: 0.0750 g (54%). M.p.: >290 °C.

Found: C 43.10; H 2.97; N 7.03%. Calc. for C₂₁H₁₉Cl₂N₃Pt: C, 43.53; H, 3.31; N, 7.25.

¹H NMR, δ_H [CD₂Cl₂]: 9.63 (d, 1H, ³J_{Pt-H} = 37 Hz, H⁶); 8.07 (t, 1H, H⁴); 7.97 (d, 1H, H⁸); 7.87 (d, 1H, H³); 7.43 (d, 1H, H⁵); 7.37 (t, H, H⁷); 7.31 (t, H, H⁵); 7.07 (s, 2H, *meta* H^{Ar}); 6.91 (t, 1H, H⁶); 2.42 (s, 3H, *para* CH₃); 2.03 (s, 6H, *ortho* CH₃).

[Pt(L⁴)Cl₂] (**8**). To a solution of K₂PtCl₄ (0.1003 g; 0.24 mmol) in H₂O (25 ml) were added L⁴ (0.0687 g; 0.24 mmol) and slowly few drops of HCl (2 M). The mixture was heated at reflux under an inert atmosphere for 72 h, until the solution was colourless, and then cooled. The yellow precipitate was filtered off, washed with water, ethanol and diethyl ether and finally recrystallised from dichloromethane and diethyl ether to give the analytical sample as a yellow solid (**8**). Yield: 0.0436g (33%). M.p.: >290 °C.

Found: C 40.97; H 2.36; N 7.51%. Calc. for C₁₉H₁₅Cl₂N₃Pt: C, 41.39; H, 2.74; N, 7.62.

¹H NMR, δ_H [CD₂Cl₂]: 9.65 (d, 1H, ³J_{Pt-H} = 38.0 Hz, H⁶); 8.02 (t, 1H, H⁴); 7.90 (t, 2H, H⁸ + H³); 7.79 (d, 1H, H⁵); 7.38–7.21 (m, 7H, H⁵ + H⁷ + H^{ar}); 6.91 (t, 1H, H⁶); 5.41 (s, 2H, CH₂).

¹H NMR, δ_H [DMSO-d₆]: 9.39 (d, br 1H, H⁶); 8.33 (m, 2H, H⁸ + H⁵); 8.22 (m, 2H, H³ + H⁴); 7.51–7.22 (m, 8H, H⁵ + H⁷ + H^{ar}); 7.12 (t, 1H, H⁶); 5.41 (s, 2H, CH₂).

[Pd(L¹)(CH₃)Cl] (**9**). To a solution of L¹ (0.0976 g; 0.36 mmol) in dichloromethane (25 ml) was added under vigorous stirring [Pd(COD)(CH₃)Cl] (0.0954 g; 0.36 mmol). The yellow solution was stirred for 24 h at room temperature then concentrated to small volume and treated with diethyl ether. The precipitate formed was filtered off, washed with diethyl ether and vacuum pumped to give the analytical sample as a yellow solid (**9**). Yield: 0.1341 g (87%).

Found: C 54.02; H 4.01; N 9.73%. Calc. for C₁₉H₁₆ClN₃Pd: C, 53.29; H, 3.77; N, 9.81.

¹H NMR, δ_H [CDCl₃]: *Major geometric isomer*: 9.11 (d, 1H, H⁶); 7.94 (d, 1H, H⁸); 7.86–7.79 (m, 3H, H³ + H⁴ + H⁵);

7.64–7.53 (m, 5H, H^{ar}); 7.24 (td, 1H, H^5); 7.18 (dd, 1H, H^7); 6.78 (t, 1H, H^6); 0.35 (s, 3H, Pd-CH₃). *Minor geometric isomer*: 8.51 (d, 1H, H^6); 7.71 (m, 5H, H^{ar}); 6.86 (t, 1H, H^6); 1.04 (s, 3H, Pd-CH₃).

[Pd(L²)(CH₃)Cl] (10). To a solution of L² (0.1030 g; 0.36 mmol) in dichloromethane (25 ml) was added under vigorous stirring [Pd(COD)(CH₃)Cl] (0.0955 g; 0.36 mmol). The yellow solution was stirred for 24 h at room temperature then concentrated to small volume and treated with diethyl ether. The precipitate formed was filtered off, washed with diethyl ether and vacuum pumped to give the analytical sample as a yellow solid (10). Yield: 0.1353 g (85%).

Found: C 54.95; H 4.61; N 9.27%. Calc. for C₂₀H₁₈ClN₃Pd: C, 54.32; H, 4.10; N, 9.50.

¹H NMR, δ_H [CDCl₃]: *Major geometric isomer*: 9.13 (d, 1H, H^6); 7.95 (d, 1H, H^8); 7.85 (m, 2H, $H^{3'} + H^4$); 7.52 (t, 1H, H^5); 7.49 (d, 1H, H^5); 7.41–7.34 (m 3H H^{ar}); 7.25 (7, 1H, H^5); 7.19 (dd, 1H, H^7); 6.78 (t, 1H, H^6); 2.41 (s, 3H, *para* CH₃); 2.02 (s, 6H, *ortho* CH₃); 0.39 (s, 3H, Pd-CH₃); 2.15 (s, 1H, *ortho* CH₃); 0.32 (s, 1H, CH₃). *Minor geometric isomer*: 8.51 (d, 1H, H^6), 2.25 (s, 1H, *ortho* CH₃); 1.00 (s, 1H, Pd-CH₃).

[Pd(L³)(CH₃)Cl] (11). To a solution of L³ (0.1131 g; 0.36 mmol) in dichloromethane (25 ml) was added under vigorous stirring [Pd(COD)(CH₃)Cl] (0.0953 g; 0.36 mmol). The yellow solution was stirred for 24 h at room temperature then concentrated to small volume and treated with diethyl ether. The precipitate formed was filtered off, washed with diethyl ether and vacuum pumped to give the analytical sample as a yellow solid (11). Yield: 0.1286 g (76%).

Found: C 56.99; H 4.97; N 8.70%. Calc. for C₂₂H₂₂ClN₃Pd: C, 56.18; H, 4.72; N, 8.93.

¹H NMR, δ_H [CDCl₃]: *Major geometric isomer*: 9.18 (d, 1H, H^6); 7.96 (d, 1H, H^8); 7.88 (m, 2H, $H^{3'} + H^4$); 7.41 (d, 1H, H^5); 7.30 (t, 1H, H^5); 7.22 (t, 1H, H^7); 7.04 (s, 2H, *meta* H); 6.79 (t, 1H, H^6); 2.41 (s, 3H, *para* CH₃); 2.02 (s, 6H, *ortho* CH₃); 0.39 (s, 3H, Pd-CH₃). *Minor geometric isomer*: 8.55 (d, 1H, H^6); 6.99 (s, 2H, *meta* H); 6.86 (t, 1H, H^6); 2.38 (s, 3H, *para* CH₃); 2.03 (s, 6H, *ortho* CH₃); 1.01 (s, 3H, Pd-CH₃).

[Pd(L⁴)(CH₃)Cl] (12). To a solution of L⁴ (0.1255 g; 0.36 mmol) in dichloromethane (25 ml) was added under vigorous stirring [Pd(COD)(CH₃)Cl] (0.0957 g; 0.36 mmol). The yellow solution was stirred for 24 h at room temperature then concentrated to small volume and treated with diethyl ether. The precipitate formed was filtered off, washed with diethyl ether and vacuum pumped to give the analytical sample as a yellow solid (12). Yield: 0.0429 g (27%).

Found: C 54.95; H 4.69; N 9.29%. Calc. for C₂₀H₁₈ClN₃Pd: C, 54.32; H, 4.10; N, 9.50.

¹H NMR, δ_H [CDCl₃]: *Major geometric isomer*: 8.56 (d, 1H, H^6); 7.89–7.80 (m, 4H, H^8 $H^{3'} + H^4 + H^5$); 7.41–7.26 (m, 5H, H^{ar}); 7.21 (t, 1H, H^7); 7.12 (dd, 1H, H^5); 6.74 (t, 1H, H^6); 5.15 (s, 2H, CH₂); 1.17 (s, 3H, Pd-CH₃). *Minor geometric isomer*: 9.23 (d, 1H, H^6); 6.75 (s, 1H, H^6); 5.36 (s, 2H, CH₂); 1.26 (s, 3H, Pd-CH₃).

[Pt(L¹)(CH₃)Cl] (13). To a solution of L¹ (0.0379 g; 0.14 mmol) in dichloromethane (25 ml) was added under vig-

orous stirring [Pt(DMSO)₂(CH₃)Cl] (0.0563 g; 0.14 mmol). The yellow solution was stirred for 72 h at room temperature then concentrated to small volume and treated with diethyl ether. The precipitate formed was filtered off, washed with diethyl ether and vacuum pumped to give the analytical sample as a yellow solid (13). Yield: 0.0528 g (73%).

Found: C 45.06; H 3.83; N 7.95%. Calc. for C₁₉H₁₆ClN₃Pt: C, 44.15; H, 3.12; N, 8.13.

¹H NMR, δ_H [CDCl₃]: *Major geometric isomer*: 9.49 (d, ³J_{Pt-H} not resolved, 1H, H^6); 8.00–7.91 (m, 2H, $H^8 + H^4$); 7.85 (d, 1H, H^5); 7.75 (d, 1H, H^3); 7.65–7.54 (m, 5H, H^{ar}); 7.30 (t, 1H, H^5); 7.22 (dd, 1H, H^7); 6.82 (t, 1H, H^6); 0.51 (s, 3H, ²J_{Pt-H} = 78.1 Hz, Pt-CH₃). *Minor geometric isomer*: 8.96 (d, ³J_{Pt-H} = 65.5 Hz 1H, H^6); 1.09 (s, 3H, ²J_{Pt-H} = 80.4 Hz, Pt-CH₃).

[Pt(L²)(CH₃)Cl] (14). To a solution of L² (0.0400 g; 0.14 mmol) in dichloromethane (25 ml) was added under vigorous stirring [Pt(DMSO)₂(CH₃)Cl] (0.0562 g; 0.14 mmol). The yellow solution was stirred for 72 h at room temperature then concentrated to small volume and treated with diethyl ether. The precipitate formed was filtered off, washed with diethyl ether and vacuum pumped to give the analytical sample as a yellow solid (14). Yield: 0.0661 g (89%).

Found: C 46.21; H 3.87; N 7.68%. Calc. for C₂₀H₁₈ClN₃Pt: C, 45.25; H, 3.42; N, 7.91.

¹H NMR, δ_H [CDCl₃]: *Major geometric isomer*: 9.50 (d, ³J_{Pt-H} not resolved, 1H, H^6); 7.99–7.92 (m, 2H, $H^8 + H^4$); 7.87 (d, 1H, H^5); 7.45 (d, 1H, H^3); 7.42–7.34 (m, 4H, H^{ar}); 7.30 (t, 1H, H^5); 7.22 (dd, 1H, H^7); 6.81 (t, 1H, H^6); 2.15 (s, 3H, CH₃); 0.51 (s, 3H, ²J_{Pt-H} = 78.1 Hz, Pt-CH₃). *Minor geometric isomer*: 8.96 (d, ³J_{Pt-H} = 65.5 Hz 1H, H^6); 2.23 (s, 3H, CH₃); 1.07 (s, 3H, ²J_{Pt-H} = 78.8 Hz, Pt-CH₃).

[Pt(L³)(CH₃)Cl] (15). To a solution of L³ (0.0377 g; 0.12 mmol) in dichloromethane (25 ml) was added under vigorous stirring [Pt(DMSO)₂(CH₃)Cl] (0.0482 g; 0.12 mmol). The yellow solution was stirred for 72 h at room temperature then concentrated to small volume and treated with diethyl ether. The precipitate formed was filtered off, washed with diethyl ether and vacuum pumped to give the analytical sample as a yellow solid (15). Yield: 0.0603 g (90%).

Found: C 48.16; H 4.29; N 7.31%. Calc. for C₂₂H₂₂ClN₃Pt: C, 47.27; H, 3.97; N, 7.52.

¹H NMR, δ_H [CD₂Cl₂]: *Major geometric isomer*: 9.43 (d, 1H, H^6). *Minor geometric isomer*: 8.71 (d, 1H, H^6); 8.12–7.89 (m, 6H); 7.50–7.21 (m, 6H); 7.08 (s, 4H, *meta* H); 6.84 (s, 2H, H^6); 2.41 (*min. st.*, s, 6H, *orto* CH₃); 2.20 (*min. st.*, s, 3H, *para* CH₃); 2.02 (*Maj. st.*, s, 6H, *orto* CH₃); 1.93 (*Maj. st.*, s, 3H, *para* CH₃); 1.15 (*min. st.*, s, 3H, ²J_{Pt-H} = 71.2 Hz, Pt-CH₃); 0.53 (*Maj. st.*, s, 3H, ²J_{Pt-H} = 71.4 Hz, Pt-CH₃).

[Pt(L⁴)(CH₃)Cl] (16). To a solution of L⁴ (0.0715 g; 0.25 mmol) in dichloromethane (25 ml) was added under vigorous stirring [Pt(DMSO)₂(CH₃)Cl] (0.1005 g; 0.25 mmol). The yellow solution was stirred for 72 h at room temperature then concentrated to small volume and treated with diethyl ether. The precipitate formed was filtered off, washed with diethyl ether and vacuum pumped to give the analytical sample as a yellow solid (16). Yield: 0.0305 g (23%). M.p. > 290 °C.

Found: C **46.17**; H **4.01**; N **7.72**%. Calc. for $C_{20}H_{18}ClN_3Pt$: C, 45.25; H, 3.42; N, 7.91.

1H NMR, δ_H [$CDCl_3$]: 9.04 (d, $^3J_{Pt-H} = 60.0$ Hz, 1H, H^6); 7.96 (t, 1H, H^4); 7.90–7.84 (m, 2H, $H^8 + H^5$); 7.76 (d, 1H, H^3); 7.44–7.24 (m, 5H, H^{ar}); 7.23–7.13 (m, 1H, $H^{5'} + H^7$); 6.81 (t, 1H, H^6); 5.30 (s, 2H, CH_2); 1.24 (s, 3H, $^2J_{Pt-H} = 80.1$ Hz, $Pt-CH_3$).

$[Pt(L^1)(CH_3)_2]$ (**17**). To a solution of L^1 (0.0732 g; 0.27 mmol) in dichloromethane (25 ml) was added under vigorous stirring $[Pt(DMSO)_2(CH_3)_2]$ (0.1030 g; 0.27 mmol). The yellow solution was stirred for 72 h at room temperature then concentrated to a small volume and treated with diethyl ether. The precipitate formed was filtered off, washed with diethyl ether and vacuum pumped to give the analytical sample as a pale green solid (**17**). Yield: 0.0616 g (46%). M.p.: 250 °C.

Found: C **49.03**; H **4.04**; N **8.29**%. Calc. for $C_{20}H_{19}N_3Pt$: C, 48.38; H, 3.86; N, 8.46.

1H NMR, δ_H [$(CD_3)_2CO$]: 9.04 (d, 1H, $^3J_{Pt-H} = 28.1$ Hz, H^6); 8.29 (d, 1H, H^8); 8.19 (t, 1H, H^4); 8.14 (d, 1H, H^3); 8.06 (d, 1H, H^5); 7.77–7.60 (m, 5H, H^{ar}); 7.34 (t, 2H, $H^{5'} + H^7$); 7.00 (t, 1H, H^6); 0.76 (s, 3H, $^2J_{Pt-H} = 90.0$ Hz, $Pt-CH_3$); 0.26 (s, 3H, $^2J_{Pt-H} = 89.4$ Hz, $Pt-CH_3$).

$[Pt(L^2)(CH_3)_2]$ (**18**). To a solution of L^2 (0.0744 g; 0.26 mmol) in dichloromethane (25 ml) was added under vigorous stirring $[Pt(DMSO)_2(CH_3)_2]$ (0.0992 g; 0.26 mmol). The yellow solution was stirred for 72 h at room temperature then concentrated to a small volume and treated with diethyl ether. The precipitate formed was filtered off, washed with diethyl ether and vacuum pumped to give the analytical sample as a pale green solid (**18**). Yield: 0.1194 g (90%). M.p.: 219 °C.

Found: C **50.05**; H **4.51**; N **8.02**%. Calc. for $C_{21}H_{21}N_3Pt$: C, 49.41; H, 4.15; N, 8.23.

1H NMR, δ_H [$(CD_3)_2CO$]: 9.03 (d, 1H, $^3J_{Pt-H} = 28.1$ Hz, H^6); 8.31 (d, 1H, H^8); 8.20 (t, 1H, H^4); 8.14 (d, 1H, H^3); 7.74 (d, 1H, H^5); 7.58–7.32 (m, 4H, H^{ar}); 7.06–6.98 (m, 2H, $H^{5'} + H^7$); 6.78 (t, 1H, H^6); 2.21 (s, 1H, CH_3); 0.75 (s, 3H, $^2J_{Pt-H} = 88.5$ Hz, $Pt-CH_3$); 0.24 (s, 3H, $^2J_{Pt-H} = 90.6$ Hz, $Pt-CH_3$).

$[Pt(L^3)(CH_3)_2]$ (**19**). To a solution of L^3 (0.0817 g; 0.26 mmol) in dichloromethane (25 ml) was added under vigorous stirring $[Pt(DMSO)_2(CH_3)_2]$ (0.0992 g; 0.26 mmol). The yellow solution was stirred for 72 h at room temperature, then concentrated to a small volume and treated with diethyl ether. The precipitate formed was filtered off, washed with diethyl ether and vacuum pumped to give the analytical sample as a pale green solid (**19**). Yield: 0.0602 g (83%). M.p.: 225 °C.

Found: C **51.97**; H **4.89**; N **7.61**%. Calc. for $C_{23}H_{25}N_3Pt$: C, 51.29; H, 4.68; N, 7.80.

1H NMR, δ_H [$(CD_3)_2CO$]: 9.03 (d, 1H, $^3J_{Pt-H} = 28.0$ Hz, H^6); 8.32 (d, 1H, H^8); 8.21 (t, 1H, H^4); 8.16 (d, 1H, H^3); 7.59 (d, 1H, H^5); 7.37–7.31 (m, 2H, $H^{5'} + H^7$); 7.08 (s, 2H, H^{ar}); 7.02 (m, 1H, H^6); 2.38 (s, 3H, *para* CH_3); 2.01 (s, 6H, *ortho* CH_3); 0.77 (s, 3H, $^2J_{Pt-H} = 88.5$ Hz, $Pt-CH_3$); 0.28 (s, 3H, $^2J_{Pt-H} = 90.6$ Hz, $Pt-CH_3$).

$[Pt(L^4)(CH_3)_2]$ (**20**). To a solution of L^4 (0.0372 g; 0.13 mmol) in acetone (25 ml) was added under vigorous stirring $[Pt(CH_3)_2(DMSO)_2]$ (0.0496 g; 0.13 mmol). The solution was stirred for 72 h at room temperature, then concentrated to a

small volume and treated with diethyl ether. The precipitate formed was filtered off, washed with diethyl ether and vacuum pumped to give the analytical sample as a pale yellow solid (**20**). (Found: C **50.51**; H **4.62**; N **8.03**%. Calc. for $C_{21}H_{21}N_3Pt$: C, 49.41; H, 4.15; N, 8.23. Yield: 0.0504 g (76%). M.p.: 227 °C.

1H NMR, δ_H [$(CD_3)_2CO$]: 9.04 (d, 1H, $^3J_{Pt-H} = 28.4$ Hz, H^6); 8.16 (pt, 2H, $H^4 + H^8$); 8.10 (d, 2H, $H^5 + H^3$); 7.44–7.26 (m, 5H, H^{ar}); 7.24–7.19 (m, 2H, $H^{5'} + H^7$); 6.91 (t, 1H, H^6); 4.90 (s, 2H, CH_2); 1.10 (s, 3H, $^2J_{Pt-H} = 87.0$ Hz, $Pt-CH_3$); 0.91 (s, 3H, $^2J_{Pt-H} = 87.9$ Hz, $Pt-CH_3$).

Computational methods

All geometry optimizations and harmonic frequency calculations were performed through Gaussian09³⁶ at DFT level of theory using the Truhlar and co-workers M06 functional³⁷ including dispersion; the SDD basis-set including f-polarization functions³⁸ and pseudo-potential has been applied for platinum while 6-311g(d,p) for the main group atoms. The solvent effect was taken into account employing the SMD continuum model of Marenich *et al.*³⁹ This level of theory describes with high accuracy the structures of second- and third-row transition metal compounds,⁴⁰ and in particular Pt and Pd organometallic complexes.⁴¹

Author contributions

Conceptualization, S.S.; Formal analysis, S.S., S.P. and A.Z.; Funding acquisition, A.Z., S.S.; Investigation, S.P., S.S., A.Z., F. O. and G.C.; Methodology, S.S., S.P. A.Z. and F.O.; Resources, A.Z., and S.S.; Software, G.S., F.O. and G.C.; Supervision, S.S., F.O.; Writing—original draft, S.S., S.P., F.O. and G.S.; Writing—review & editing, S.S., S.P., A.Z., F.O., G.S. and G.C.; All authors have read and agreed to the published version of the manuscript.

Conflicts of interest

The authors declare no conflict of interest. The funders had no role in the design of the study; in the collection, analyses, or interpretation of data; in the writing of the manuscript, or in the decision to publish the results.

Acknowledgements

Financial support from Università degli Studi di Sassari is gratefully acknowledged (“Fondo di Ateneo per la Ricerca 2020”: S. S. and A. Z.). F. O. would like to acknowledge Dr Chris Muryn, the X-ray service at the Department of Chemistry, University of Manchester, and the Engineering and Physical Sciences Research Council (Grant EP/K039547/1) for support.

References

- (a) C. Kaes, A. Katz and M. W. Hosseini, *Chem. Rev.*, 2000, **100**(10), 3553–3590; (b) A. Bencini and V. Lippolis, *Coord. Chem. Rev.*, 2010, **254**, 2096–2180; (c) E. C. Constable and C. E. Housecroft, *Molecules*, 2019, **24**, 3951 and references therein; (d) L. Calvanese, M. E. Cucciolito, A. D'Amora, G. D'Auria, A. Esposito, R. Esposito, L. Falcigno and F. Ruffo, *Eur. J. Inorg. Chem.*, 2015, 4068–4075; (e) A. Annunziata, A. Amoresano, M. E. Cucciolito, R. Esposito, G. Ferraro, I. Iacobucci, P. Imbimbo, R. Lucignano, M. Melchiorre, M. Monti, C. Scognamiglio, A. Tuzi, D. M. Monti, A. Merlino and F. Ruffo, *Inorg. Chem.*, 2020, **59**, 4002–4014.
- (a) W. Cabri, I. Candiani, A. Bedeschi and R. Santi, *Synlett*, 1992, 871; (b) C. Bolm, M. Zehnder and D. Bur, *Angew. Chem., Int. Ed. Engl.*, 1990, **29**, 205–207; (c) C. Bolm, M. Ewald, M. Felder and G. Schlingloff, *Chem. Ber.*, 1992, **125**, 1169–1190.
- B. Liu, W.-L. Yu, J. Pei, S.-Y. Liu, Y.-H. Lai and W. Huang, *Macromolecules*, 2001, **34**, 7932–7940.
- J. Mathieu, B. Fraisse, D. Lacour, N. Ghermani, F. Montaigne and A. Marsura, *Eur. J. Inorg. Chem.*, 2006, 133–136.
- U. S. Schubert, J. L. Kersten, A. E. Pemp, C. D. Eisenbach and G. R. Newkome, *Eur. J. Org. Chem.*, 1998, 2573–2581.
- V. Balzani and A. Juris, *Coord. Chem. Rev.*, 2001, **211**, 97–115.
- S. Margel, W. Smith and F. C. Anson, *J. Electrochem. Soc.*, 1978, **125**, 241–246.
- (a) G. Minghetti, M. A. Cinellu, S. Stoccoro, G. Chelucci and A. Zucca, *Inorg. Chem.*, 1990, **29**, 5138; (b) G. Minghetti, M. A. Cinellu, S. Stoccoro, A. Zucca and M. Manassero, *J. Chem. Soc., Dalton Trans.*, 1995, 777; (c) A. Zucca, M. A. Cinellu, M. V. Pinna, S. Stoccoro and G. Minghetti, *Organometallics*, 2000, **19**, 4295; (d) A. Zucca, S. Stoccoro, M. A. Cinellu, G. Minghetti, M. Manassero and M. Sansoni, *Eur. J. Inorg. Chem.*, 2002, 3336; (e) G. Minghetti, S. Stoccoro, M. A. Cinellu, B. Soro and A. Zucca, *Organometallics*, 2003, **22**, 4770; (f) A. Zucca, S. Stoccoro, M. A. Cinellu, G. L. Petretto and G. Minghetti, *Organometallics*, 2007, **26**, 5621; (g) O. A. Filippov, V. A. Kirkina, N. V. Belkova, S. Stoccoro, A. Zucca, G. M. Babakhina, L. M. Epstein and E. S. Shubina, *Z. Phys. Chem.*, 2013, **227**(6–7), 869; (h) F. Cocco, A. Zucca, S. Stoccoro, M. Serratrice, A. Guerri and M. A. Cinellu, *Organometallics*, 2014, **33**, 3414; (i) S. Stoccoro, L. Maidich, T. Ruiu, M. A. Cinellu, G. J. Clarkson and A. Zucca, *Dalton Trans.*, 2015, **44**(41), 18001–18011; (j) L. Maidich, M. A. Cinellu, F. Cocco, S. Stoccoro, M. Sedda, S. Galli and A. Zucca, *J. Organomet. Chem.*, 2016, **819**, 76.
- G. Hajos and Z. Riedl, *Sci. Synth.*, 2002, **12**, 613.
- (a) A. G. Ligtenbarg, A. L. Spek, R. Hage and B. L. Feringa, *J. Chem. Soc., Dalton Trans.*, 1999, 659; (b) M. E. Bluhm, M. Ciesielski, O. Walter, H. Görls and M. Döring, *Inorg. Chem.*, 2003, **42**, 8878.
- E. Yamaguchi, F. Shibahara and T. Murai, *J. Org. Chem.*, 2011, **76**, 6146–6158, and references therein.
- (a) M. Nakatsuka and T. Shimamura, *Jpn. Kokai Tokkyo Koho*, JP 2001035664, 2001; M. Nakatsuka and T. Shimamura, *Chem. Abstr.*, 2001, **134**, 170632 (b) G. Tominaga, R. Kohama and A. Takano, *Jpn. Kokai Tokkyo Koho*, JP 2001006877, 2001; G. Tominaga, R. Kohama and A. Takano, *Chem. Abstr.*, 2001, **134**, 93136 (c) D. Kitazawa, G. Tominaga and A. Takano, *Jpn. Kokai Tokkyo Koho*, JP 2001057292, 2001. D. Kitazawa, G. Tominaga and A. Takano, *Chem. Abstr.*, 2001, **134**, 200276.
- H. Nakamura and H. Yamamoto, *PCT Int. Appl.*, WO 2005043630, 2005; H. Nakamura and H. Yamamoto, *Chem. Abstr.*, 2005, **142**, 440277.
- (a) L. Salassa, A. Albertino, C. Garino, G. Volpi, C. Nervi, R. Gobetto and K. I. Hardcastle, *Organometallics*, 2008, **27**, 1427–1435; (b) C. Garino, T. Ruiu, L. Salassa, A. Albertino, G. Volpi, C. Nervi, R. Gobetto and K. I. Hardcastle, *Eur. J. Inorg. Chem.*, 2008, 3587–3591.
- (a) G. Volpi, E. Priola, C. Garini, A. Daolio, R. Rabezzana, P. Benzi, A. Giordana, E. Diana and R. Gobetto, *Inorg. Chim. Acta*, 2020, 509; (b) G. A. Ardizzoia, S. Brenna, S. Durini, B. Therrien and M. Veronelli, *Eur. J. Inorg. Chem.*, 2014, 4310–4319; (c) G. A. Ardizzoia, S. Brenna, S. Durini and B. Therrien, *Polyhedron*, 2015, **90**, 214–220.
- S. Durini, G. A. Ardizzoia, B. Therrien and S. Brenna, *New J. Chem.*, 2017, **41**, 3006–3014.
- N. Kundu, S. M. T. Abtab, S. Kundu, A. Endo, S. J. Teat and M. Chaudhury, *Inorg. Chem.*, 2012, **51**, 2652–2661.
- A. L. Guckian, M. Doering, M. Ciesielski, O. Walter, J. Hjelm, N. M. O'Boyle, W. Henry, W. R. Browne, J. J. McGarvey and J. G. Vos, *Dalton Trans.*, 2004, 3943–3949.
- (a) K. P. Thakor, M. V. Lunagariya, B. S. Bhatt and M. N. Patel, *Luminescence*, 2019, **34**, 113–124; (b) L. Ronconi and P. J. Sadler, *Coord. Chem. Rev.*, 2007, **251**, 1633–1648.
- (a) B. Butschke and H. Schwarz, *Chem. Sci.*, 2012, **3**, 308; (b) A. Zucca, G. L. Petretto, S. Stoccoro, M. A. Cinellu, M. Manassero, C. Manassero and G. Minghetti, *Organometallics*, 2009, **28**, 2150–2159; (c) A. Zucca, L. Maidich, M. I. Pilo, S. Pischedda, M. Sedda and S. Stoccoro, *Appl. Sci.*, 2020, **10**, 6665; (d) A. Zucca and M. I. Pilo, *Molecules*, 2021, **26**, 328.
- D. A. Kanthecha, B. S. Bhatt and M. N. Patel, *Heliyon*, 2019, **5**, e01968.
- (a) J. Wang, L. Dyers Jr., R. Mason Jr., P. Amoyaw and X. R. Bu, *J. Org. Chem.*, 2005, **70**, 2353–2356; (b) J. Wang, R. Mason, D. Van Derveer, K. Feng and X. R. Bu, *J. Org. Chem.*, 2003, **68**, 2415–2418.
- R. Grigg, P. Kennewell, V. Savic and V. Sridharan, *Tetrahedron*, 1992, **47–48**, 10423–10430.
- S. Albano, G. Olivo, L. Mandolini, C. Massera, F. Ugozzoli and S. Di Stefano, *J. Org. Chem.*, 2017, **82**, 3820–3825.

- 25 Z. Hu, J. Hou, J. Liu, W. Yu and J. Chang, *Org. Biomol. Chem.*, 2018, **16**, 5653–5660.
- 26 (a) A. D. Ryabov, *Chem. Rev.*, 1990, **90**, 403; (b) M. Albrecht, *Chem. Rev.*, 2010, **110**, 576.
- 27 P. K. Byers and A. J. Canty, *Organometallics*, 1990, **9**, 210–220.
- 28 E. Constable, R. P. G. Henney, T. A. Leese and D. A. Tocher, *J. Chem. Soc., Chem. Commun.*, 1990, 513–515.
- 29 (a) J. E. Huheey, E. A. Keiter and R. L. Keiter, in *Inorganic Chemistry: Principles of Structure and Reactivity*, Harper Collins, New York, USA, 4th edn, 1993; (b) J. B. Mann, T. L. Meek, E. T. Knight, J. F. Capitani and L. C. Allen, *J. Am. Chem. Soc.*, 2000, **122**, 5132–5137.
- 30 A. Abo-Amer, M. S. McCready, F. Zhang and R. J. Puddephatt, *Can. J. Chem.*, 2012, **90**, 46–54 and references therein.
- 31 S. Shil, D. Bhattacharya, S. Sarkar and A. Misra, Performance of the Widely Used Minnesota Density Functionals for the Prediction of Heat of Formations, Ionization Potentials of Some Benchmarked First Row Transition Metal Complexes, *J. Phys. Chem. A*, 2013, **117**(23), 4945–4955.
- 32 A. I. Vogel, *Vogel's Textbook of Practical Organic Chemistry*, Longman Scientific and Technical, Harlow, UK, 5th edn, 1989.
- 33 R. E. Riilke, J. M. Ernsting, A. L. Spek, C. J. Elsevier, P. W. N. M. van Leeuwen and K. Vrieze, *Inorg. Chem.*, 1993, **32**, 5769–5778.
- 34 (a) C. Eaborn, K. Kundu and A. J. Pidcock, *J. Chem. Soc., Dalton Trans.*, 1981, 933–938; (b) R. Romeo and L. Monsù Scolaro, *Inorg. Synth.*, 1998, **32**, 153; (c) R. Romeo, L. Monsù Scolaro, N. Nastasi, B. E. Mann, G. Bruno and F. Nicolo, *Inorg. Chem.*, 1996, **35**, 7691.
- 35 E. A. Baquero, A. Rodríguez-Zúñiga, J. C. Flores, M. Temprado and E. de Jesús, *J. Organomet. Chem.*, 2019, **896**, 108–112.
- 36 M. J. Frisch, G. W. Trucks, H. B. Schlegel, G. E. Scuseria, M. A. Robb, J. R. Cheeseman, G. Scalmani, V. Barone, B. Mennucci, G. A. Petersson, H. Nakatsuji, M. Caricato, X. Li, H. P. Hratchian, A. F. Izmaylov, J. Bloino, G. Zheng, J. L. Sonnenberg, M. Hada, M. Ehara, K. Toyota, R. Fukuda, J. Hasegawa, M. Ishida, T. Nakajima, Y. Honda, O. Kitao, H. Nakai, T. Vreven, J. A. Montgomery Jr., J. E. Peralta, F. Ogliaro, M. Bearpark, J. J. Heyd, E. Brothers, K. N. Kudin, V. N. Staroverov, T. Keith, R. Kobayashi, J. Normand, K. Raghavachari, A. Rendell, J. C. Burant, S. S. Iyengar, J. Tomasi, M. Cossi, N. Rega, J. M. Millam, M. Klene, J. E. Knox, J. B. Cross, V. Bakken, C. Adamo, J. Jaramillo, R. Gomperts, R. E. Stratmann, O. Yazyev, R. Austin, R. Cammi, C. Pomelli, J. W. Ochterski, R. L. Martin, K. Morokuma, V. G. Zakrzewski, G. A. Voth, P. Salvador, J. J. Dannenberg, S. Dapprich, A. D. Daniels, Ö. Farkas, J. B. Foresman, J. V. Ortiz, J. Cioslowski and D. J. Fox, *Gaussian 09, revision D.01*, Gaussian, Inc., Wallingford, CT, 2010.
- 37 (a) Y. Zhao and D. G. Truhlar, The M06 suite of density functionals for main group thermochemistry, thermochemical kinetics, noncovalent interactions, excited states, and transition elements: two new functionals and systematic testing of four M06-class functionals and 12 other functionals, *Theor. Chem. Acc.*, 2008, **120**(1), 215–241; (b) Y. Zhao and D. G. Truhlar, A new local density functional for main-group thermochemistry, transition metal bonding, thermochemical kinetics, and noncovalent interactions, *J. Phys. Chem.*, 2006, **125**(19), 194101.
- 38 A. Ehlers, M. Böhme, S. Dapprich, A. Gobbi, A. Höllwarth, V. Jonas, K. Köhler, R. Stegmann, A. Veldkamp and G. Frenking, A set of f-polarization functions for pseudopotential basis sets of the transition metals Sc-Cu, Y-Ag and La-Au, *Chem. Phys. Lett.*, 1993, **208**(1–2), 111–114.
- 39 A. V. Marenich, C. J. Cramer and D. G. Truhlar, Universal Solvation Model Based on Solute Electron Density and on a Continuum Model of the Solvent Defined by the Bulk Dielectric Constant and Atomic Surface Tensions, *J. Phys. Chem. B*, 2009, **113**(18), 6378–6396.
- 40 (a) C. J. Cramer and D. G. Truhlar, Density functional theory for transition metals and transition metal chemistry, *Phys. Chem. Chem. Phys.*, 2009, **11**(46), 10757–10816; (b) Y. Minenkov, A. Singstad, G. Occhipinti and V. R. Jensen, The accuracy of DFT-optimized geometries of functional transition metal compounds: a validation study of catalysts for olefin metathesis and other reactions in the homogeneous phase, *Dalton Trans.*, 2012, **41**(18), 5526–5541.
- 41 E. A. C. Bushnell and R. J. Boyd, Assessment of Several DFT Functionals in Calculation of the Reduction Potentials for Ni-, Pd-, and Pt-Bis-ethylene-1,2-dithiolene and -Diselenolene Complexes, *J. Phys. Chem. A*, 2015, **119**(5), 911–918.